Bioorganic Chemistry 92 (2019) 103304

Contents lists available at ScienceDirect

Bioorganic Chemistry

journal homepage: www.elsevier.com/locate/bioorg

Novel pyridazinone derivatives as butyrylcholinesterase inhibitors

Yasemin Dundar[a,*], Ozge Kuyrukcu[a], Gokcen Eren[a], F. Sezer Senol Deniz[b], Tijen Onkol[a], Ilkay Erdogan Orhan[b]

[a] Department of Pharmaceutical Chemistry, Faculty of Pharmacy, Gazi University, 06330 Ankara, Turkey
[b] Department of Pharmacognosy, Faculty of Pharmacy, Gazi University, 06330 Ankara, Turkey

ARTICLE INFO

Keywords:
Alzheimer's disease
Pyridazinone derivatives
Acetylcholinesterase inhibitors
Butyrylcholinesterase inhibitors
Docking

ABSTRACT

In the current study, forty-four new [3-(2/3/4-methoxyphenyl)-6-oxopyridazin-1(6*H*)-yl]methyl carbamate derivatives were synthesized and evaluated for their ability to inhibit electric eel acetylcholinesterase (*Ee*AChE) and equine butyrylcholinesterase (eqBuChE) enzymes. According to the inhibitory activity results, [3-(2-methoxyphenyl)-6-oxopyridazin-1(6*H*)-yl]methyl heptylcarbamate (**16c**, eqBuChE, IC_{50} = 12.8 μM; *Ee*AChE, no inhibition at 100 μM) was the most potent eqBuChE inhibitor among the synthesized compounds and was found to be a moderate inhibitor compared to donepezil (eqBuChE, IC_{50} = 3.25 μM; *Ee*AChE, IC_{50} = 0.11 μM). Kinetic and molecular docking studies indicated that compounds **16c** and **14c** (hexylcarbamate derivative, eqBuChE, IC_{50} = 35 μM; *Ee*AChE, no inhibition at 100 μM) were mixed-type inhibitors which accommodated within the catalytic active site (CAS) and peripheral anionic site (PAS) of hBuChE through stable hydrogen bonding and π-π stacking. Furthermore, it was determined that [3-(2-methoxyphenyl)-6-oxopyridazin-1(6*H*)-yl]methyl (4-methylphenyl)carbamate **7c** (eqBuChE, IC_{50} = 34.5 μM; *Ee*AChE, 38.9% inhibition at 100 μM) was the most active derivative against *Ee*AChE and a competitive inhibitor binding to the CAS of hBuChE. As a result, 6-(2-methoxyphenyl)pyridazin-3(2*H*)-one scaffold is important for the inhibitory activity and compounds **7c**, **14c** and **16c** might be considered as promising lead candidates for the design and development of selective BuChE inhibitors for Alzheimer's disease treatment.

1. Introduction

Dementia is a cognitive impairment syndrome which affects memory, cognitive abilities, and behavior. According to the World Health Organization, there are approximately 50 million dementia patients globally and this number is estimated to grow to 152 million by 2050. The most common form of dementia is Alzheimer's disease (AD), accounting for about 60–70% of cases [1,2]. AD, an irreversible neurodegenerative disorder, leads to the progressive loss of cognitive and intellectual function, reduced ability to perform the activities of daily living as well as the emergence of behavioral and psychological symptoms such as depression, apathy, anxiety, agitation, irritability, delusion, and hallucination [3,4]. There is no cure for AD at the moment, where people aged 65 and older survive an average of 4–8 years after diagnosis of Alzheimer's type of dementia [5].

Neuropathological features of the AD are characterized by amyloidal plaques, neurofibrillary tangles, cholinergic neurons damage, and abnormally decreased levels of the acetylcholine (ACh). Most of the current drugs for the AD are mainly based on enhancing cholinergic neurotransmission through inhibition of acetylcholinesterase (AChE) enzyme that hydrolyses ACh. The AChE inhibitors donepezil, rivastigmine, and galantamine are used for symptomatic treatment for mild-to-moderate AD [6–8]. In the later stages of AD, the level of AChE enzyme progressively decreases due to dramatic cholinergic synapse and neuronal loss. However, the butyrylcholinesterase (BuChE) levels increase significantly and BuChE plays a critical role for ACh hydrolysis in the late stage of AD [9–11]. In addition, both enzymes, in particular, BuChE, are also found to associate with neurotoxic amyloid β plaques and neurofibrillary tangles in human AD brain tissue [12,13]. Thus, in recent years, studies on selective BuChE inhibitors have been increased and are considered as an alternative for the treatment of patients with mild-to-late stages of AD [9–11,14,15].

In our previous work, [3-(4-substitutedphenyl)-6-oxopyridazin-1(6*H*)-yl)methyl phenylcarbamate derivatives were synthesized and screened for their inhibitory activity on cholinesterase enzymes. Among the compounds, [3-(4-methoxyphenyl)-6-oxopyridazin-1(6*H*)-yl)methyl phenylcarbamate derivative showed inhibitory activity against both AChE and BuChE [16]. Previous studies by different research

* Corresponding author.
E-mail address: yasemina@gazi.edu.tr (Y. Dundar).

https://doi.org/10.1016/j.bioorg.2019.103304
Received 30 May 2019; Received in revised form 16 September 2019; Accepted 17 September 2019
Available online 18 September 2019

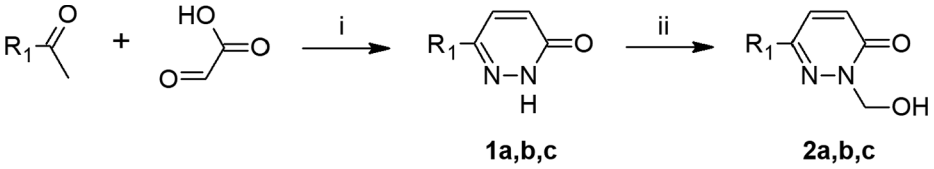

Scheme 1. Reagents and conditions: i) 105–108 °C, 3 h; then $NH_2NH_2{\cdot}H_2O$, reflux, 2 h. ii) 37% formalin, reflux, 2 h. R_1: 4-methoxyphenyl (a, 1st serie); 3-methoxyphenyl (b, 2nd serie); 2-methoxyphenyl (c, 3rd serie).

groups have shown that the arylcarbamate or long chain alkylcarbamate group is a suitable fragment to achieve selective BuChE inhibition [15,17–20]. Based on these findings, in order to obtain more potent and selective BuChE inhibitors, [3-(2/3/4-methoxyphenyl)-6-oxopyridazin-1(6*H*)-yl)methyl substitutedphenyl/ alkylcarbamate derivatives were synthesized and evaluated for their inhibitory effects on *Ee*AChE and eqBuChE enzymes. Additionally, kinetic and molecular docking studies were performed for the selected compounds.

2. Results and discussion

2.1. Chemistry

The synthetic routes for the target compounds are outlined in Schemes 1 and 2. The starting compounds, 6-(substitutedphenyl)pyridazin-3(2*H*)-one derivatives (**1a, 1b, 1c**) was readily prepared by the reaction of glyoxylic acid monohydrate, appropriate acetophenone, and hydrazine hydrate. These compounds were then reacted with formaldehyde to obtain hydroxymethyl derivatives (**2a, 2b, 2c**) as shown in Scheme 1. The compounds except *N*-methyl and *N*,*N*-dimethyl carbamate derivatives were afforded by the reaction of hydroxymethyl derivatives with appropriate isocyanate in the presence of *N*-methylimidazole (Scheme 2). Methylamine and 1,1-carbonyldiimidazole were used instead of toxic methyl isocyanate in the synthesis of *N*-methyl carbamate derivatives (**8a, 8b, 8c**) (Scheme 2). *N*,*N*-dimethylcarbamate derivatives (**17a, 17b, 17c**) were prepared by the reaction of *N*,*N*-dimethylcarbamoyl chloride, hydroxymethyl derivatives, and *N*-methylimidazole (Scheme 2).

2.2. AChE and BuChE inhibitory activity

Inhibitory activities of the synthesized compounds on *Ee*AChE and eqBuChE were evaluated by Ellman's method [21–23]. The results are given as the percentage of enzyme inhibition at 100 μM (Fig. 1). IC_{50} values were calculated for compounds which exhibited inhibition of more than 50% (Table 1). Donepezil and galantamine were used as the reference compounds tested at 10 μM concentration.

According to the activity results, in the first serie (**3a-17a**) bearing 6-(4-methoxyphenyl)pyridazin-3(2*H*)-one moiety; all compounds except **6a** (4.6%) and **14a** (20.1%) had no inhibitory effect on *Ee*AChE at 100 μM. Concerning the activity of this serie against eqBuChE, the inhibitory activity remained below 15% in the aromatic, short alkyl chain, and dimethyl carbamate derivatives (**3a-11a, 17a**). The significant increase in activity was observed with butyl derivative (**12a**, 27.5%). The pentyl (**13a**), hexyl (**14a**), cyclohexyl (**15a**) derivatives showed inhibitory activity of 36.4%, 48.9%, 51.5% (IC_{50} = 97.2 μM), respectively. However, the heptyl derivative (**16a**) exerted an inhibitory activity of 33.2% (Fig. 1).

On the other hand, the activity results of the second serie bearing 6-(3-methoxyphenyl)pyridazin-3(2*H*)-one moiety were evaluated; only 4-fluorophenylcarbamate (**4b**, 11.1%), 4-methoxyphenylcarbamate (**6b**, 5.9%) and hexylcarbamate (**14b**, 16.6%) derivatives had inhibitory effect on *Ee*AChE. Regarding the activity of this serie against eqBuChE, similar to the first serie, the aromatic, short alkyl chain, and dimethyl carbamate derivatives (**3b-11b, 17b**) showed no inhibitory activity or less than 15%. An increase in activity was observed with butyl derivative (**12b**) which showed 20.9% inhibition. Pentyl (**13b**), hexyl (**14b**), and cyclohexyl (**15b**) derivatives exhibited 49.4%, 55.0% (IC_{50} = 76.1 μM), and 43.0% inhibitory activity, respectively. The heptyl derivative (**16b**) was tested at 50 μM due to the solubility problem and showed the inhibitory activity of 31.9% at this concentration (Fig. 1).

The third serie carrying 6-(2-methoxyphenyl)pyridazin-3(2*H*)-one moiety is the group with the most active compounds. According to the results of *Ee*AChE inhibition assay; only phenyl (**3c**), 4-chlorophenyl (**5c**), 4-methoxyphenyl (**6c**), and 4-methylphenyl (**7c**) derivatives showed 24.7%, 15.4%, 38.2% and 38.9% inhibitory activity, respectively. As far as the activity against eqBuChE is concerned, methyl to butyl chain and dimethyl carbamate derivatives (**8c-12c**) showed less than 15% inhibitory activity. The activity increased as the chain extended, that pentyl (**13c**), hexyl (**14c**), cyclohexyl (**15c**), heptyl (**16c**) derivatives showed with 49.5% (IC_{50} = 99.4 μM), 68.4% (IC_{50} = 35.0 μM), 38.2%, 76.9% (IC_{50} = 12.8 μM) inhibitory activity, respectively. Different from the other series, the aromatic carbamate

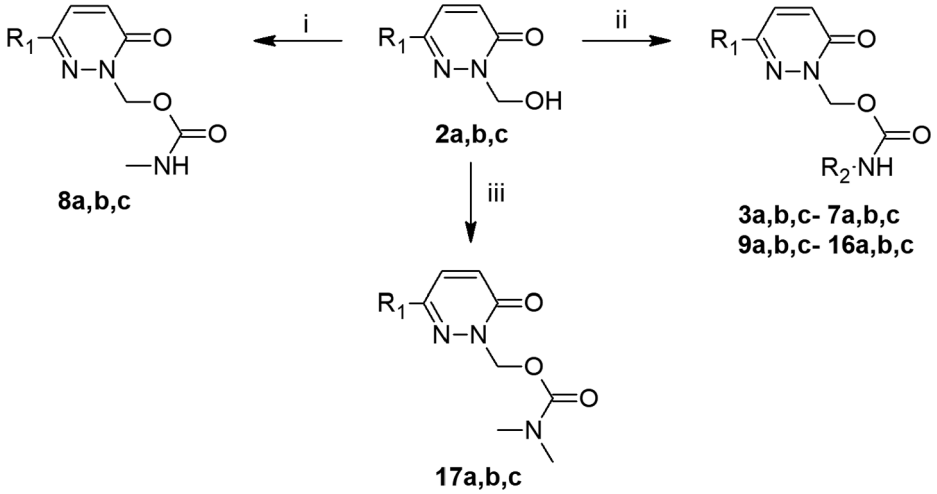

Scheme 2. Reagents and conditions: i) CDI, AcCN, rt, 3 h; then CH_3NH_2, K_2CO_3, rt, 3 h. ii) appropriate isocyanate, NMI, AcCN, rt, 24 h. iii) DMCC, NMI, K_2CO_3, AcCN, rt, 24 h.

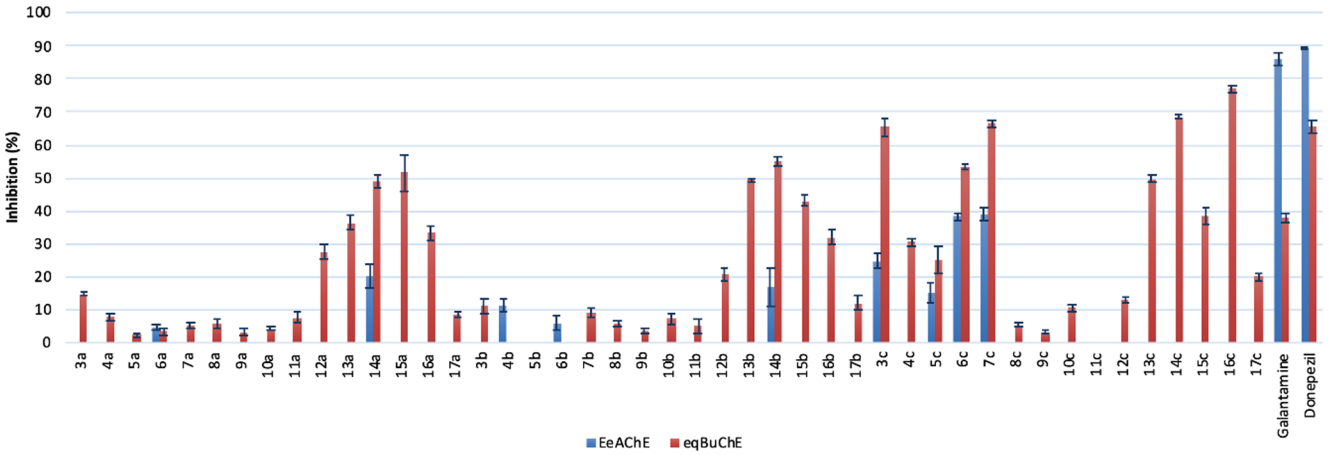

Fig. 1. *Ee*AChE and eqBuChE inhibitory activity of the synthesized compounds (**3a-17a**, **3b-17b**, **3c-17c**) and the references. Data are indicated as percentage of inhibition at 100 μM ± SD (n = 4). Donepezil and galantamine were used as the reference drugs at 10 μM concentration.

derivatives were also found to display inhibitory activity on eqBuChE. The phenyl (**3c**), 4-fluorophenyl (**4c**), 4-chlorophenyl (**5c**), 4-methoxyphenyl (**6c**), and 4-methylphenyl (**7c**) carbamate derivatives showed 65.4% (IC_{50} = 50.3 μM), 30.4%, 25.0%, 53.4% (IC_{50} = 92.6 μM), and 66.6% (IC_{50} = 34.5 μM), respectively (Fig. 1).

In generally, the synthesized compounds exhibited a better inhibitory activity against eqBuChE compared with *Ee*AChE. However, none of the compounds was found to be more active than references donepezil and galantamine. When the structure-activity relationships were evaluated for eqBuChE, the position of the methoxy substituent in the phenylpyridazinone ring was found to be important, and it was suggested that the presence of ortho methoxy group increased the inhibitory activity. Regarding the importance of the substituent in carbamate group, especially, long-chain carbamate groups such as hexyl or heptyl was enhanced the eqBuChE inhibitory activity. Although the heptyl carbamate derivative **16c** was the most active eqBuChE inhibitor among the synthesized compounds, it was four-fold less active than donepezil. Butyl chain was the critical length at which inhibitory activity begins increasing significantly. Regarding the third serie, among the substituted aromatic carbamate derivatives, electron withdrawing groups like fluoro (**4c**), chloro (**5c**) groups decreased inhibitory activity while improvement in activity was observed in the following order: methyl (**7c**) > H (**3c**) > methoxy (**6c**) group. Compound **7c** was found to be 2.6 fold more active than **6c** against eqBuChE. Besides, compounds **6c** (38.2%) and **7c** (38.9%) derivatives showed similar activity pattern in *Ee*AChE.

For the eqBuChE inhibition mechanism of the selected compounds **7c**, **14c**, and **16c** was determined by enzyme kinetic study. The Lineweaver-Burk plots and replots of the slope versus concentration were utilized to obtain the inhibition constant (K_i) (Table 1 and Fig. 2). Compound **7c**, 4-methylphenylcarbamate derivative, displayed a competitive inhibition while hexylcarbamate derivative **14c** and heptylcarbamate derivative **16c** showed a mixed-type inhibition. The obtained K_i values were consistent with the measured IC_{50} values. Obtained plots of the inhibitors are shown in Fig. 2.

To elucidate the time dependent inhibition, the IC_{50} shift assay was carried out by pre-incubating the eqBuChE with (i) no compound, (ii) selected compounds, and (iii) rivastigmine as the reference compound for different time periods (40, 20, 10 min). Rivastigmine, the pseudo-irreversible inhibitor, showed time-dependent inhibition with 3.1 fold shift in IC_{50}. In case of tested compounds, compound **7c**, **14c** and **16c** exhibited similar inhibition profile with 1.47, 1.8, and 2.8 fold shift IC_{50}

Table 1
*Ee*AChE and eqBuChE inhibitory activity of the selected compounds and references.

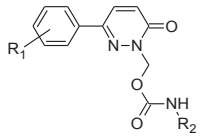

Comp.	R_1	R_2	*Ee*AChE		eqBuChE			
			Inhibition (%)[a]	IC_{50} (μM)	Inhibition (%)[a]	IC_{50} (μM)	K_i (μM)	Inhibition mechanism
15a	4-OCH_3	cyclohexyl	ni[b]	nd[c]	51.5 ± 5.6	97.2 ± 0.6		
14b	3-OCH_3	hexyl	16.6 ± 5.8	nd	55.0 ± 1.2	76.1 ± 2.5		
3c	2-OCH_3	phenyl	24.7 ± 2.2	nd	65.4 ± 2.7	50.3 ± 3.4		
6c	2-OCH_3	4-methoxyphenyl	38.2 ± 1.0	nd	53.4 ± 0.9	92.6 ± 4.0		
7c	2-OCH_3	4-methylphenyl	38.9 ± 2.1	nd	66.6 ± 1.0	34.5 ± 3.2	33.3	Competitive
13c	2-OCH_3	pentyl	ni	nd	49.5 ± 1.0	99.4 ± 0.3		
14c	2-OCH_3	hexyl	ni	nd	68.4 ± 0.4	35.0 ± 2.6	30.2	Mixed-type
16c	2-OCH_3	heptyl	ni	nd	76.9 ± 1.2	12.8 ± 0.8	12.0	Mixed-type
Donepezil[d]			89.1 ± 0.1	0.11 ± 0.03	65.5 ± 1.8	3.25 ± 0.16		
Galantamine[d]			86.0 ± 2.1	3.7 ± 0.5	37.9 ± 1.2	nd		

[a] Data are indicated as percentage of inhibition at 100 μM ± SD (n = 4).
[b] ni: no inhibition.
[c] nd: not determined.
[d] Donepezil and galantamine were used as the reference drugs at 10 μM concentration.

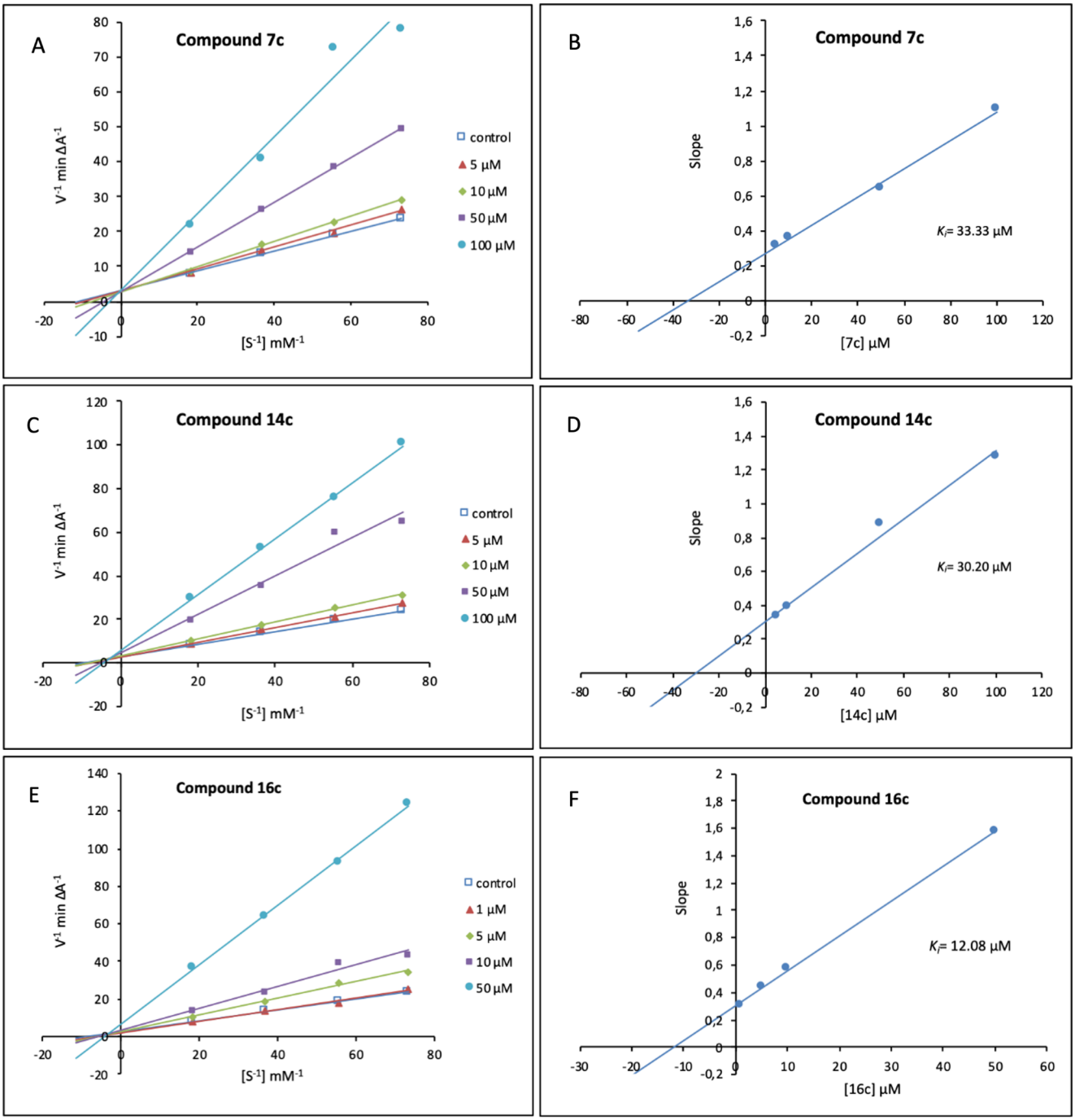

Fig. 2. Kinetic study on the mechanism of eqBuChE inhibition by **7c, 14c,** and **16c**. Lineweaver-Burk plots: **7c** (A), **14c** (C), **16c** (E). Slope replot vs inhibitor concentration: **7c** (B), **14c** (D), **16c** (F).

values, respectively. The time-dependent decrease in IC_{50} values of the compounds suggested that our compounds may be a reversible inhibitor or a pseudo-irreversible inhibitor or an irreversible inhibitor. Although carbamate derivatives are generally known to inhibit ChEs by a mechanism involving covalent interaction between their carbamate group and the catalytic serine, our compounds do not participate this type of interaction with active site serine. However, being an irreversible or a pseudo-irreversible inhibitor could not be suggested for the compounds **7c**, **14c** and **16c**. Therefore, our compounds were proposed as reversible with tight-binding inhibition [24,25] which is known to show kinetics similar to covalent inhibition may the explanation for the binding mechanism for the compounds tested.

2.3. Molecular docking studies

To explore possible binding interactions of potential inhibitors, compounds **14b**, **3c**, **6c**, **7c**, **14c**, and **16c** were selected to dock into *Ee*AChE (PDB: 1C2O), hAChE (PDB: 4EY7), and hBuChE (PDB: 4TPK) using Glide module implemented in Schrödinger Small-Molecule Drug Discovery Suite.

The compounds showing dual inhibition of AChE and BuChE fit into the binding site of *Ee*AChE interacting with the CAS and PAS regions. In the case of compounds **3c**, **6c**, and **7c**, the 2-methoxyphenyl ring was bound to the PAS, forming π-π stacking interactions with TRP286. The pyridazinone and phenyl rings adjacent to the carbamate moiety extended beyond the CAS and stabilized by a hydrogen bond between

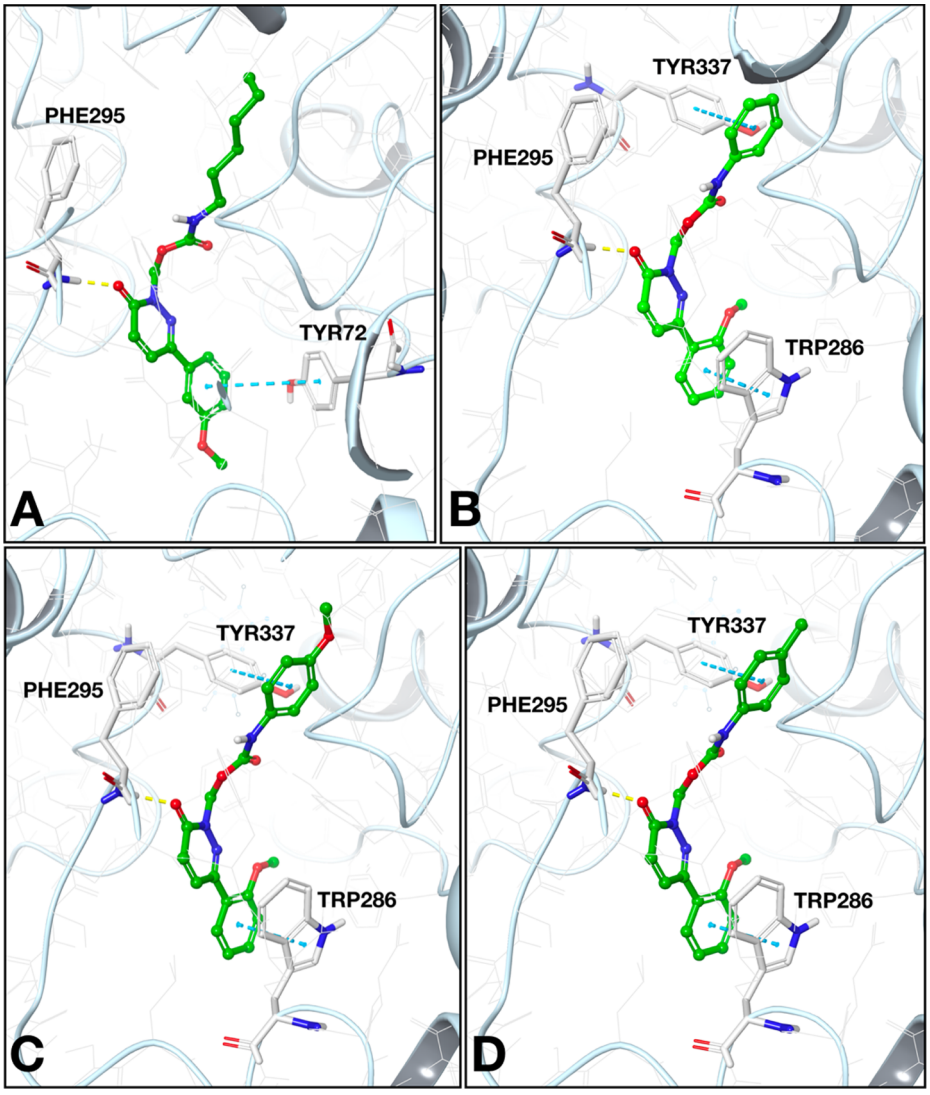

Fig. 3. Proposed binding modes for compounds **14b** (A), **3c** (B), **6c** (C), and **7c** (D) in *Ee*AChE active site (PDB: 1C2O). The compounds are presented as green ball and sticks with nitrogen and oxygen atoms in blue and red, respectively. The involved residues are named and showed as white sticks. Hydrogen bonds and π-π stacking contacts are represented with yellow and cyan dashed lines, respectively.

carbonyl oxygen and PHE295 backbone and π-π stacking contacts with TYR337, respectively. For compound **14b**, the interactions obtained were a π-π stacking contact between 3-methoxyphenyl ring and TYR72 from the PAS and a hydrogen bond between carbonyl oxygen and PHE295 backbone. Unlike the compounds **3c**, **6c**, and **7c**, compound **14b** showed no contact with TYR337 from the CAS due to replacement of the ring with alkyl chain (Fig. 3).

Since the X-ray crystal structures of *Ee*AChE do not contain any water molecules, the selected compounds were also docked into hAChE in order to identify the impact of water molecules on binding pattern as shown in Fig. 4. Considering large mobility of some residues to accommodate ligands [26] in AChE structures, the flexibility of some side chains such as TRP286, PHE338 have been taken into account in docking studies by Schrödinger's Induced Fit Docking (IFD) protocol [27]. The results demonstrated that keeping the structural water molecules in active site provided favorable hydrogen bonds with TYR124 for all compounds and SER293 for compound **6c**. For compound **14b** anchored the PAS via TRP286 instead of TYR72 in *Ee*AChE. The carbonyl oxygen of carbamate moiety formed a hydrogen bond with TYR124 from the PAS through HOH954. The PAS interaction of the compound **3c** with TRP286 was replaced with TYR124 *via* HOH737 mediated hydrogen bond in *Ee*AChE. In the case of compound **6c**, the orientation of the molecule differed from the proposed binding mode in *Ee*AChE active site. 4-Methoxyphenyl moiety positioned in the mouth of the gorge by a π-π stacking contact with TRP286 and a water mediated hydrogen bond with SER293 whereas the pyridazinone ring formed a π-π stacking contact with TYR337 from oxyanion hole. Besides, additional hydrogen bonds were observed between the PAS residue TYR124 and the carbonyl oxygen of the carbamate group and oxygen atom of 2-methoxyphenyl ring through water network. Regarding compound **7c**, the presence of water molecules provided a hydrogen bond with TYR124. Moreover, additional π-π stacking contacts which enhanced the stability of inhibitor:enzyme complex compared to *Ee*AChE were observed in the PAS and the oxyanion hole with TYR341 and TRP86, respectively.

Although enzyme inhibition studies were performed by eqBuChE, molecular docking studies were carried out using hBuChE since there is no available x-ray structure of eqBuChE. According to molecular docking results performed with hBuChE, orientation of the compounds was mainly driven by the interactions with the CAS comprising residues. Unlike the obtained binding modes in AChE, none of the compounds interacted with the PAS residues except compound **3c**.

As depicted in Fig. 5, the binding mode of compound **14b** suggested that the pyridazinone moiety was bound to choline binding site by a π-π

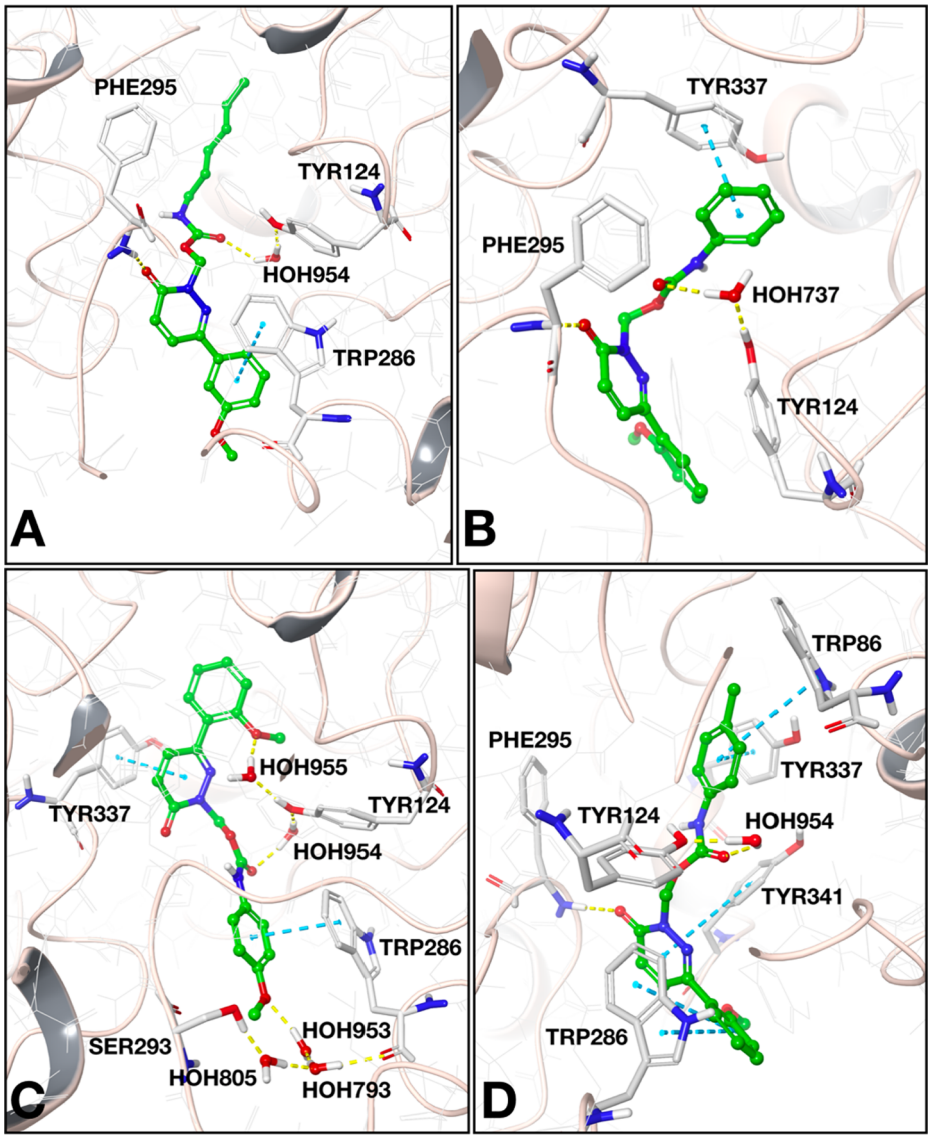

Fig. 4. Proposed binding modes for compounds **14b** (A), **3c** (B), **6c** (C), and **7c** (D) in hAChE active site (PDB: 4EY7). The compounds are presented as green ball and sticks with nitrogen and oxygen atoms in blue and red, respectively. The involved residues and structural water molecules are named and showed as white sticks. Hydrogen bonds and π-π stacking contacts are represented with yellow and cyan dashed lines, respectively.

stacking contact with TRP82. 3-Methoxyphenyl ring was oriented toward THR120 which was located between choline binding site and the PAS forming a hydrogen bond, whereas another hydrogen bond was observed between nitrogen atom of carbamate group and ALA328. Compound **3c** was found to be the one among the all compounds tested that bound to the PAS by interacting ASP70 *via* water network. In addition to this, water mediated hydrogen bonds with SER79, the catalytic triad member SER198, GLY117 from oxyanion hole, and THR120 and a π-π stacking contact with PHE329 were found to be important for the stabilization of inhibitor:enzyme complex. In the case of compound **6c**, 2-methoxyphenyl ring was located in the pocket forming acyl binding site and oxyanion hole π-π stacking contacts with TRP231 and PHE329, respectively. A hydrogen bond between carbonyl oxygen of carbamate group and THR120 was also observed. The compound **7c** was found to be interacted with only oxyanion hole by forming π-π stacking contacts with TRP82 and PHE329.

Molecular docking results considering glide scores and the residues interacted were found to be in accordance with *in vitro* data obtained. The distances between carbamate moiety of the compounds and catalytic triad member SER203 that ranges from 6.22 Å to 6.40 Å were measured for the compounds, but none of them showed proximity to SER203 (Tables 2 and 3).

The compounds **14c** and **16c** exhibited inhibitory potency for only BuChE occupied the region between anionic site and acyl pocket (Fig. 6). Both compounds bound to oxyanion hole *via* π-π stacking contact between 2-methoxyphenyl ring and PHE329 and water mediated hydrogen bond with GLY117, while forming a hydrogen bond between oxygen atom of pyridazinone moiety and THR120. Both compounds interacted the catalytic triad member SER198 through water mediated hydrogen bond. However, the orientation of compound **14c** allowed to form hydrogen bonds with SER79 and ASP70 from the PAS by water network which was not observed for compound **16c** and the π-π stacking contact with TRP231 was observed for only compound **16c**.

Molecular docking results obtained showed that there is a good correlation between predicted binding modes and BuChE inhibition of the compounds tested regarding glide scores and the residues interacted and the carbamate group of the compounds was not sufficiently close to react with catalytic triad member SER198 (Table 4).

As depicted in Fig. 7A, the compounds **7c**, **14c**, and **16c,** which

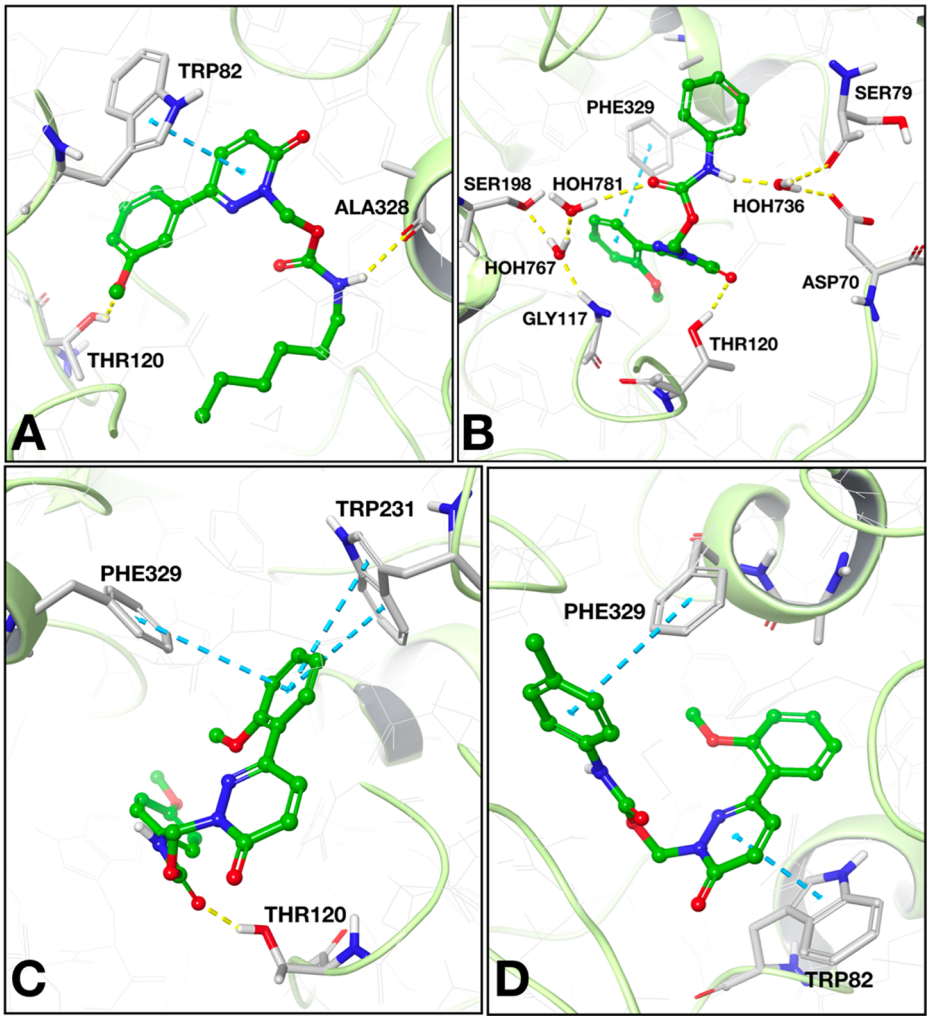

Fig. 5. Proposed binding modes for compounds **14b** (A), **3c** (B), **6c** (C), and **7c** (D) in hBuChE active site (PDB: 4TPK). The compounds are presented as green ball and sticks with nitrogen and oxygen atoms in blue and red, respectively. The involved residues and structural water molecules are named and showed as white sticks. Hydrogen bonds and π-π stacking contacts are represented with yellow and cyan dashed lines, respectively.

Table 2
Molecular interaction of *Ee*AChE active site with the compounds docked.

Comp.	Glide score (kcal/mol)	Interacting residues	Distance carbamate-SER203 (Å)
14b	−6.615	TYR72 (π-π stack); PHE295 (H-bond)	6.40
3c	−7.586	TRP286, TYR337 (π-π stack); PHE295 (H-bond)	6.22
6c	−7.450	TRP286, TYR337 (π-π stack); PHE295 (H-bond)	6.32
7c	−7.791	TRP286, TYR337 (π-π stack); PHE295 (H-bond)	6.39

exhibited the highest inhibitory effect against hBuChE among the compounds tested, preferred to occupy the CAS region between oxyanion hole and acyl binding site. Kinetic studies revealed that compound **7c** was a competitive inhibitor, while compounds **14c** and **16c** were mixed-type inhibitors of hBuChE. Molecular docking studies were in good agreement with kinetic studies since the competitive inhibitor **7c** interacted with CAS and the mixed-type inhibitor **14c** exerted a dual CAS-PAS binding. Although the interaction with the PAS was not observed for mixed-type inhibitor **16c**, its orientation of nitrogen atom of carbamate moiety which interacted the PAS residue was found to be very similar to that of compound **14c**.

Although similarities between AChE and BuChE active sites regarding the shape and the residue arrangement were available, BuChE has a larger catalytic site than AChE [28,29] (Fig. 7B). Therefore, this structural difference was suggested to rationalize the observed lacking *in vitro* AChE inhibition over BuChE, for instance compounds **14c** and **16c**. Compound **14c** selectively inhibiting BuChE with respect to AChE, bound to hBuChE in U-shaped conformation while having less contracted pose in AChE active site. If compound **14c** binds to AChE in the same conformation as in BuChE, it would lead to clashes between the alkyl chain and residues PHE295 and PHE297. Due to steric hindrance, compound **14c** preferred a linear conformation in AChE active site through only π-π contacts between terminal phenyl ring and TRP286, the PAS region residue. Due to having alkyl chain instead of aromatic rings as in compounds **14b**, **3c**, **6c**, **7c**, there is lack of π-π interaction which leads less stable enzyme:inhibitor complex for BuChE inhibitors compared to that of the compounds exhibited dual inhibition. It is also observed that there is an agreement with the chain length and inhibition% values for BuChE. Increased chain length might help compound to transfer into a flexible conformation in order to occupy the larger active site of BuChE. Finally, bearing alkyl chain that enables the U-shaped conformation may enhance the BuChE selectivity over AChE.

Table 3
Molecular interaction of hAChE active site with the compounds docked.

Comp.	Glide score (kcal/mol)	Interacting residues	Distance carbamate-SER203 (Å)
14b	−8.815	TRP286 (π-π stack); PHE295 (H-bond); TYR124 (HOH954 mediated H-bond)	9.38
3c	−9.576	TYR337 (π-π stack); PHE295 (H-bond); TYR124 (HOH737 mediated H-bond)	9.43
6c	−10.290	TRP286, TYR337 (π-π stack); TYR124 (HOH954, HOH955 mediated H-bond); TRP286 (HOH953, HOH793 mediated H-bond); SER293 (HOH953, HOH793, HOH805 mediated H-bond)	10.97
7c	−10.025	TRP86, TRP286, TYR337, TYR341 (π-π stack); PHE295 (H-bond); TYR124 (HOH954 mediated H-bond)	8.62

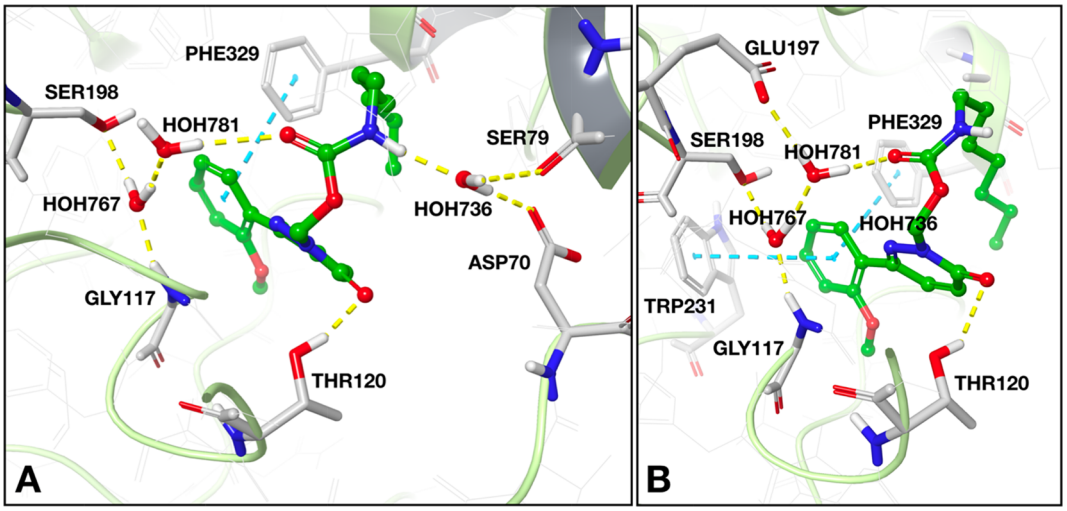

Fig. 6. Proposed binding modes for compounds **14c** (A), **16c** (B) in hBuChE active site (PDB: 4TPK). The compounds are presented as green ball and sticks with nitrogen and oxygen atoms in blue and red, respectively. The involved residues and structural water molecules are named and showed as white sticks. Hydrogen bonds and π-π stacking contacts are represented with yellow and cyan dashed lines, respectively.

Table 4
Molecular interaction of hBuChE active site with the compounds docked.

Comp.	Glide score (kcal/mol)	Interacting residues	Distance carbamate-SER198 (Å)
14b	−6.879	TRP82 (π-π stack); THR120, ALA328 (H-bond)	9.67
3c	−7.704	PHE329 (π-π stack); THR120 (H-bond); GLY117, SER198 (HOH781, HOH767 mediated H-bond); ASP70, SER79 (HOH736 mediated H-bond)	8.86
6c	−7.815	TRP231, PHE329 (π-π stack); THR120 (H-bond)	8.61
7c	−7.921	TRP82, PHE329 (π-π stack)	6.52
14c	−7.850	PHE329 (π-π stack); THR120 (H-bond); ASP70, SER79 (HOH736 mediated H-bond); GLY117, SER198 (HOH781, HOH767 mediated H-bond)	8.87
16c	−8.664	TRP231, PHE329 (π-π stack); THR120 (H-bond); GLU197 (HOH781 mediated H-bond); GLY117, SER198 (HOH781, HOH767 mediated H-bond)	7.98

3. Conclusion

In this paper, three series of (6-oxo-3-substitutedpyridazin-1(6*H*)-yl) methyl carbamate derivatives were synthesized and evaluated for their ability to inhibit *Ee*AChE and eqBuChE. All compounds except **6a, 4b**, and **6b**, displayed inhibitory activity against eqBuChE. It is observed that the compounds with short alkyl chain were not active in all series, while the long-chain carbamate derivatives showed a significant eqBuChE inhibitory activity. Only in the third serie, aromatic carbamate derivatives **3c, 6c, 7c** exhibited inhibitory activity against both *Ee*AChE and eqBuChE. Besides, it is determined that the presence of the 6-(2-methoxyphenyl)pyridazin-3(2*H*)-one moiety increased the inhibitory activity. In total, eight compounds showed 50% or more inhibitory activity for eqBuChE and IC_{50} values were calculated. Among these compounds, **15a, 13c, 14c,** and **16c** were inhibited solely eqBuChE at tested concentration. The heptylcarbamate derivative **16c** (IC_{50} = 12.8 μM) was found to be the most active compound. For the determination of the inhibitory mechanism, **7c, 14c,** and **16c** were selected for enzyme kinetic study. Obtained results indicated that compound **7c** was a competitive inhibitor, while compounds **14c** and **16c** were mixed-type inhibitors of eqBuChE. Additionally, K_i values of the selected compounds were consistent with the IC_{50} values. Molecular docking results also supported the findings from kinetic study in which the competitive inhibitor **7c** interacted with CAS and the mixed-type inhibitor **14c** exerted a dual CAS-PAS binding. Although the interaction with the PAS was not observed for mixed-type inhibitor **16c**, its

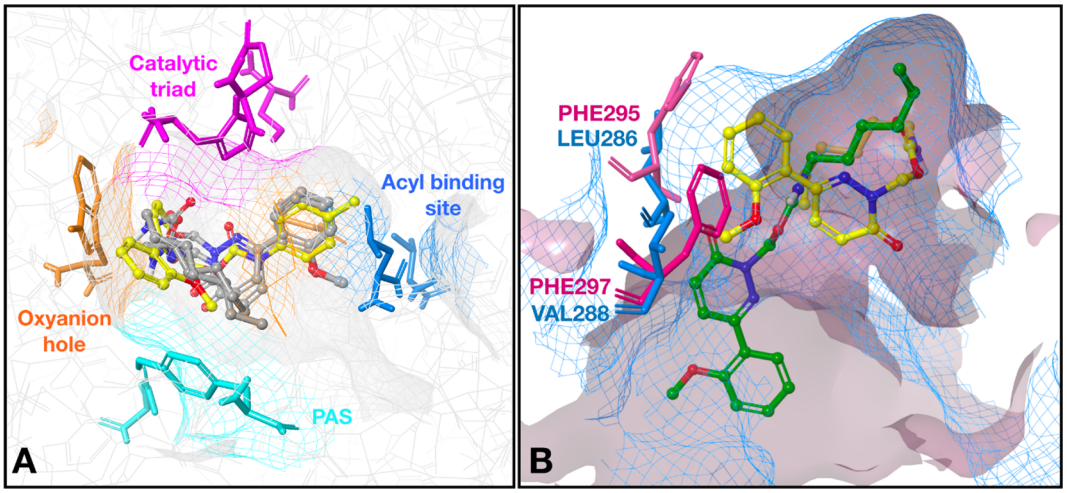

Fig. 7. (A) The superimposition of docked compounds **7c** (yellow), **14c** (grey), and **16c** (grey) inside hBuChE active site (PDB: 4TPK). All compounds are presented as ball and stick with nitrogen and oxygen atoms in blue and red, respectively. Residues of acyl binding pocket, oxyanion hole, PAS and catalytic triad are shown in blue, orange, cyan and magenta sticks, respectively. (B) Superimposed binding modes of compound **14c** inside hAChE (green) and hBuChE (yellow) active sites. External surfaces of hAChE and hBuChE gorge cavities are presented as pink solid and blue mesh, respectively. The key residues of hAChE are colored pink, while the corresponding residues are colored blue.

orientation of nitrogen atom of carbamate moiety which interacted the PAS residue was found to be very similar to that of compound **14c**. According to the IC_{50} shift assay, compounds **7c, 14c,** and **16c** exhibited a time-dependent inhibition against eqBuChE. Although the time-dependent inhibition of compounds showed similarity with that of rivastigmine, molecular docking studies indicated that compounds do not inhibit eqBuChE by a mechanism involving covalent bond formation at the active site serine. A reversible with tight-binding inhibition of eqBuChE which is known to show kinetics similar to covalent irreversible inhibitors was proposed as a binding mechanism for the compounds tested because of the π-π stacking interactions with especially PHE329. In conclusion, these compounds could be considered as promising lead candidates for the design and development of drugs against AD.

4. Experimental part

4.1. Chemistry

All reagents and solvents were purchased from Sigma-Aldrich and used without further purification. Melting points were determined with an Electrothermal-9200 Digital Melting Point Apparatus and were uncorrected. ^{1}H NMR and ^{13}C NMR spectra were recorded in DMSO-d_6 on a Varian Mercury 400, 400 MHz High Performance Digital FT-NMR spectrometer at the NMR facility of Faculty of Pharmacy, Ankara University. All chemical shifts were recorded as δ (ppm). Microanalyses for C, H, and N were performed on a Leco-932 at Faculty of Pharmacy, Ankara University, and they were within the range of ± 0.4% of the theoretical value. HRMS spectra were taken on a Waters LCT Premier XE orthogonal acceleration time-of-flight (oa-TOF) mass spectrometer using ESI (+) or ESI (−) methods. The synthesis of the compounds **1a** [30], **2a** [31], **3a** [16], **1b** [30], **1c** [30] were previously reported.

4.1.1. General procedure for the synthesis of 6-substitutedpyridazin-3(2H)-one derivatives (1a, 1b, 1c)

The mixture of glyoxylic acid monohydrate (5.52 g, 0.06 mol) and appropriate acetophenone derivative (27.04 g, 0.18 mol) was heated at 105–108 °C for 3 h. At the end of the time, the reaction medium was cooled to room temperature and to added 24 mL of water and 4.8 mL of conc. ammonium hydroxide. Then, the mixture was extracted with dichloromethane (2 × 50 mL), and 2.9 mL (0.06 mol) hydrazine hydrate was added onto the separated aqueous phase. The mixture was heated under reflux for 2 h. At the end of the period, the reaction medium was cooled, the precipitate was filtered and crystallized from the appropriate solvent.

4.1.2. General procedure for the synthesis of 2-(hydroxymethyl)-6-substitutedpyridazin-3(2H)-one derivatives (2a, 2b, 2c)

A mixture of 5.05 g (0.025 mol) of 6-substitutedpyridazin-3(2*H*)-one (**1a**, **1b**, **1c**) and 30 mL of 37% formalin was heated under reflux for 2 h. At the end of the period, the reaction medium was cooled to room temperature, 30 mL water was added, and the precipitated product was washed with water and filtered.

4.1.3. General procedure for the synthesis of carbamate derivatives (3a, 3b, 3c-7a, 7b, 7c and 9a, 9b, 9c-16a, 16b, 16c)

Appropriate isocyanate derivative (0.001 mol) and *N*-methylimidazole (0.016 mL, 0.016 g, 0.0002 mol) were added to mixture of 2-(hydroxymethyl)-6-substitutedpyridazin-3(2*H*)-one derivative (**2a**, **2b**, **2c**) (0.23 g, 0.001 mol) in 10 mL acetonitrile. The mixture was stirred at room temperature for 24 h. Then 50 mL ice-water was added, precipitated product was filtered, and crystallized from the appropriate solvent.

4.1.4. General procedure for the synthesis of N-methylcarbamate derivatives (8a, 8b, 8c)

The mixture of 2-(hydroxymethyl)-6-substitutedpyridazin-3(2*H*)-one derivative (**2a**, **2b**, **2c**) (0.269 g, 0.00116 mol) and 1,1-carbonyldiimidazole (0.379 g, 0.00234 mol) in 10 mL acetonitrile was stirred at room temperature for 3 h. Then potassium carbonate (0.160 g, 0.00116 mol) and methylamine (0.066 mL, 30% aqueous solution, 0.059 g, 0.00116 mol) was added to reaction mixture and stirred at room temperature for 3 h. At the end of the time, reaction mixture was poured into 50 mL of ice-water; the precipitate formed was filtered and crystallized from the appropriate solvent.

4.1.5. General procedure for the synthesis of N,N-dimethylcarbamate derivatives (17a, 17b, 17c)

To mixture of 2-(hydroxymethyl)-6-substitutedpyridazin-3(2*H*)-one derivative (**2a**, **2b**, **2c**) (0.23 g, 0.001 mol), *N*-methylimidazole (0.016 mL, 0.016 g, 0.0002 mol) and potassium carbonate (0.138 g, 0.001 mol) in 10 mL acetonitrile was added dimethylcarbamoyl chloride (0.09 mL, 0.107 g, 0.001 mol) and stirred at room temperature for 24 h. At the end of the time, reaction mixture poured into 50 mL ice/

water, obtained product was filtered and purified by preparative TLC in dichloromethane:methanol (100:3) solvent system.

4.1.5.1. 6-(4-Methoxyphenyl)pyridazin-3(2H)-one, 1a. Crystallized from water to yield 58.2%; m.p. 194 °C; HRMS calc. for $C_{11}H_{11}N_2O_2$ [M + H]: 203.0821, found: 203.0828 [30].

4.1.5.2. 2-(Hydroxymethyl)-6-(4-methoxyphenyl)pyridazin-3(2H)-one, 2a. The crude product was used without further purification due to the stability problem. Yield 86.2%; m.p. 145 °C; HRMS calc. for $C_{12}H_{13}N_2O_3$ [M + H]: 233.0926, found: 233.0932 [31].

4.1.5.3. [3-(4-Methoxyphenyl)-6-oxopyridazin-1(6H)-yl]methyl phenylcarbamate, 3a [16]. Crystallized from acetonitrile to yield 82.6%; m.p. 198 °C; ^{1}H NMR (DMSO-d_6) δ: 9.91 (1H, s, NH), 8.05 (1H, d, *J:* 9.6 Hz, pyridazine H5), 7.83 (2H, d, *J:* 9.2 Hz, phenyl H2,6), 7.45 (2H, d, *J:* 8 Hz, phenyl H2′,6′), 7.26 (2H, t, phenyl H3′,5′), 7.09 (1H, d, *J:* 10 Hz, pyridazine H4), 7.02 (2H, d, *J:* 8.8 Hz, phenyl H3,5), 6.98 (1H, t, phenyl H4′), 6.07 (2H, s, CH_2), 3.78 (3H, s, OCH_3) ppm; ^{13}C NMR (DMSO-d_6) δ: 160.48, 158.78, 151.96, 144.07, 138.56, 131.76, 130.33, 128.73, 127.37, 126.15, 122.70, 118.24, 114.28, 72.92, 55.23 ppm; Anal. calc. for $C_{19}H_{17}N_3O_4.3/4H_2O$: C, 62.54; H, 5.11; N, 11.52, found: C, 62.32; H, 4.89; N, 11.39%; HRMS calc. for $C_{19}H_{18}N_3O_4$ [M + H]: 352.1297, found: 352.1296.

4.1.5.4. [3-(4-Methoxyphenyl)-6-oxopyridazin-1(6H)-yl]methyl (4-fluorophenyl)carbamate, 4a. Crystallized from acetonitrile to yield 70.4%; m.p. 212 °C; ^{1}H NMR (DMSO-d_6) δ: 9.95 (1H, s, NH), 8.06 (1H, d, *J:* 9.6 Hz, pyridazine H5), 7.82 (2H, d, *J:* 9.2 Hz, phenyl H2,6), 7.44 (2H, dd, J_1: 8.8 Hz, J_2: 5.2 Hz, phenyl H2′,6′), 7.13–7.07 (3H, m, pyridazine H4, phenyl H3′,5′), 7.02 (2H, d, *J:* 8.8 Hz, phenyl H3,5), 6.06 (2H, s, CH_2), 3.78 (3H, s, OCH_3) ppm; ^{13}C NMR (DMSO-d_6) δ: 160.54, 158.83, 157.81 (d, *J:* 238 Hz, F-phenyl H4′), 152.11, 144.14, 134.96, 131.86, 130.40, 127.42, 126.20, 119.98, 115.39 (d, *J:* 22.5 Hz, F-phenyl H3′,5′), 114.35, 73.02, 55.29 ppm; Anal. calc. for $C_{19}H_{16}FN_3O_4$: C, 61.79; H, 4.37; N, 11.38, found: C, 61.81; H, 4.523; N, 11.46%; HRMS calc. for $C_{19}H_{17}FN_3O_4$ [M + H]: 370.1203, found: 370.1204.

4.1.5.5. [3-(4-Methoxyphenyl)-6-oxopyridazin-1(6H)-yl]methyl (4-chlorophenyl)carbamate, 5a. Crystallized from acetonitrile to yield 77.6%; m.p. 217 °C; ^{1}H NMR (DMSO-d_6) δ: 10.06 (1H, s, NH), 8.07 (1H, d, *J:* 10 Hz, pyridazine H5), 7.82 (2H, d, *J:* 8.8 Hz, phenyl H2,6), 7.46 (2H, d, *J:* 8.8 Hz, phenyl H2′,6′), 7.32 (2H, d, *J:* 9.2 Hz, phenyl H3′,5′), 7.09 (1H, d, *J:* 9.6 Hz, pyridazine H4), 7.02 (2H, d, *J:* 8.8 Hz, phenyl H3,5), 6.06 (2H, s, CH_2), 3.78 (3H, s, OCH_3) ppm; ^{13}C NMR (DMSO-d_6) δ: 160.55, 158.84, 151.96, 144.16, 137.64, 131.88, 130.40, 128.72, 127.43, 126.43, 126.18, 119.76, 114.35, 73.10, 55.30 ppm; Anal. calc. for $C_{19}H_{16}ClN_3O_4$: C, 59.15; H, 4.18; N, 10.89, found: C, 58.86; H, 4.290; N, 10.97%; HRMS calc. for $C_{19}H_{17}ClN_3O_4$ [M + H]: 386.0908, found: 386.0909.

4.1.5.6. [3-(4-Methoxyphenyl)-6-oxopyridazin-1(6H)-yl]methyl (4-methoxyphenyl)carbamate, 6a. Crystallized from acetonitrile to yield 74%; m.p. 210 °C; ^{1}H NMR (DMSO-d_6) δ: 9.71 (1H, s, NH), 8.06 (1H, d, *J:* 10 Hz, pyridazine H5), 7.82 (2H, d, *J:* 8.8 Hz, phenyl H2,6), 7.34 (2H, d, *J:* 8 Hz, phenyl H2′,6′), 7.07 (1H, d, *J:* 10.4 Hz, pyridazine H4), 7.02 (2H, d, *J:* 8.4 Hz, phenyl H3,5), 6.84 (2H, d, *J:* 8.8 Hz, phenyl H3′,5′), 6.04 (2H, s, CH_2), 3.78 (3H, s, OCH_3), 3.67 (3H, s, OCH_3) ppm; ^{13}C NMR (DMSO-d_6) δ: 160.53, 158.83, 154.99, 152.13, 144.09, 131.81, 131.60, 130.39, 127.42, 126.22, 119.86, 114.35, 114.00, 72.90, 55.29, 55.14 ppm; Anal. calc. for $C_{20}H_{19}N_3O_5$: C, 62.99; H, 5.02; N, 11.02, found: C, 62.86; H, 5.154; N, 10.96%; HRMS calc. for $C_{20}H_{20}N_3O_5$ [M + H]: 382.1403, found: 382.1404.

4.1.5.7. [3-(4-Methoxyphenyl)-6-oxopyridazin-1(6H)-yl]methyl (4-methylphenyl)carbamate, 7a. Crystallized from ethanol/water to yield 44%; m.p. 213 °C; ^{1}H NMR (DMSO-d_6) δ: 9.82 (1H, s, NH), 8.09 (1H, d, *J:* 9.6 Hz, pyridazine H5), 7.86 (2H, d, *J:* 9.2 Hz, phenyl H2,6), 7.35 (2H, d, *J:* 8 Hz, phenyl H2′,6′), 7.12–7.04 (5H, m, pyridazine H4, phenyl H3,5, phenyl H3′,5′), 6.08 (2H, s, CH_2), 3.81 (3H, s, OCH_3), 2.23 (3H, s, CH_3) ppm; ^{13}C NMR (DMSO-d_6) δ: 160.53, 158.84, 152.00, 144.11, 136.05, 131.83, 131.65, 130.40, 129.18, 127.43, 126.22, 118.32, 114.35, 72.91, 55.30, 20.30 ppm; Anal. calc. for $C_{20}H_{19}N_3O_4$: C, 65.74; H, 5.24; N, 11.50; found: C, 66.10; H, 5.426; N, 11.52%; HRMS calc. for $C_{20}H_{20}N_3O_4$ [M + H]: 366.1454, found: 366.1457.

4.1.5.8. [3-(4-Methoxyphenyl)-6-oxopyridazin-1(6H)-yl]methyl methylcarbamate, 8a. Crystallized from acetone/water to yield 54.8%; m.p. 155 °C; ^{1}H NMR (DMSO-d_6) δ: 8.04 (1H, d, *J:* 9.6 Hz, pyridazine H5), 7.81 (2H, d, *J:* 9.2 Hz, phenyl H2,6), 7.27 (1H, q, NH), 7.06–7.01 (3H, m, pyridazine H4, phenyl H3,5), 5.92 (2H, s, CH_2), 3.79 (3H, s, OCH_3), 2.57 (3H, d, CH_3) ppm; ^{13}C NMR (DMSO-d_6) δ: 160.50, 158.76, 155.22, 143.91, 131.68, 130.34, 127.39, 126.28, 114.33, 72.76, 55.30, 26.89 ppm; Anal. calc. for $C_{14}H_{15}N_3O_4$: C, 58.13; H, 5.23; N, 14.53; found: C, 58.29; H, 5.382; N, 14.49%; HRMS calc. for $C_{14}H_{16}N_3O_4$ [M + H]: 290.1141, found: 290.1131.

4.1.5.9. [3-(4-Methoxyphenyl)-6-oxopyridazin-1(6H)-yl]methyl ethylcarbamate, 9a. Crystallized from ethanol/water to yield 73.85%; m.p. 80 °C; ^{1}H NMR (DMSO-d_6) δ: 8.04 (1H, d, *J:* 9.6 Hz, pyridazine H5), 7.81 (2H, d, *J:* 9.2 Hz, phenyl H2,6), 7.39 (1H, t, NH), 7.06–7.01 (3H, m, pyridazine H4, phenyl H3,5), 5.91 (2H, s, CH_2), 3.79 (3H, s, OCH_3), 3.01–2.98 (2H, m, CH_2), 0.98 (3H, t, CH_3) ppm; ^{13}C NMR (DMSO-d_6) δ: 160.50, 158.76, 154.51, 143.91, 131.68, 130.35, 127.40, 126.28, 114.33, 72.62, 55.30, 35.06, 14.84 ppm; Anal. calc. for $C_{15}H_{17}N_3O_4.1/2H_2O$: C, 57.68; H, 5.81; N, 13.45; found: C, 57.36; H, 6.123; N, 13.42%; HRMS calc. for $C_{15}H_{18}N_3O_4$ [M + H]: 304.1297, found: 304.1288.

4.1.5.10. [3-(4-Methoxyphenyl)-6-oxopyridazin-1(6H)-yl]methyl propylcarbamate, 10a. Crystallized from acetone/water to yield 84.6%; m.p. 101 °C; ^{1}H NMR (DMSO-d_6) δ: 8.04 (1H, d, *J:* 10 Hz, pyridazine H5), 7.81 (2H, d, *J:* 9.2 Hz, phenyl H2,6), 7.41 (1H, t, NH), 7.06–7.01 (3H, m, pyridazine H4, phenyl H3,5), 5.91 (2H, s, CH_2), 3.79 (3H, s, OCH_3), 2.92 (2H, q, CH_2), 1.40–1.35 (2H, m, CH_2), 0.79 (3H, t, CH_3) ppm; ^{13}C NMR (DMSO-d_6) δ: 160.49, 158.76, 154.72, 143.91, 131.67, 130.34, 127.39, 126.27, 114.32, 72.62, 55.29, 42.02, 22.47, 11.15 ppm; Anal. calc. for $C_{16}H_{19}N_3O_4.1/2H_2O$: C, 58.89; H, 6.18; N, 12.88; found: C, 59.04; H, 6.384; N, 12.99%; HRMS calc. for $C_{16}H_{20}N_3O_4$ [M + H]: 318.1454, found: 318.1451.

4.1.5.11. [3-(4-Methoxyphenyl)-6-oxopyridazin-1(6H)-yl]methyl propan-2-ylcarbamate, 11a. The crude product was purified by preparative TLC using dichloromethane-methanol (100:3) solvent system. Yield 49.9%; m.p. 77 °C; ^{1}H NMR (DMSO-d_6) δ: 8.05 (1H, d, *J:* 9.6 Hz, pyridazine H5), 7.82 (2H, d, *J:* 9.2 Hz, phenyl H2,6), 7.35 (1H, d, NH), 7.07–7.02 (3H, m, pyridazine H4, phenyl H3,5), 5.91 (2H, s, CH_2), 3.79 (3H, s, OCH_3), 3.62–3.57 (1H, m, CH), 1.01 (6H, d, CH_3) ppm; ^{13}C NMR (DMSO-d_6) δ: 160.49, 158.76, 153.81, 143.90, 131.65, 130.33, 127.38, 126.27, 114.32, 72.52, 55.30, 42.39, 22.38 ppm; Anal. calc. for $C_{16}H_{19}N_3O_4.3/4H_2O$: C, 58.08; H, 6.25; N, 12.70, found: C, 58.14; H, 6.076; N, 12.32%; HRMS calc. for $C_{16}H_{20}N_3O_4$ [M + H]: 318.1454, found: 318.1443.

4.1.5.12. [3-(4-Methoxyphenyl)-6-oxopyridazin-1(6H)-yl]methyl butylcarbamate, 12a. Crystallized from ethanol/water to yield 60.6%; m.p. 72 °C; ^{1}H NMR (DMSO-d_6) δ: 8.05 (1H, d, *J:* 10 Hz, pyridazine H5), 7.82 (2H, d, *J:* 9.2 Hz, phenyl H2,6), 7.40 (1H, t, NH), 7.07–7.01 (3H, m, pyridazine H4, phenyl H3,5), 5.92 (2H, s, CH_2), 3.79 (3H, s, OCH_3), 2.97 (2H, q, CH_2), 1.37–1.33 (2H, m, CH_2), 1.26–1.22 (2H, m, CH_2), 0.82 (3H, t, CH_3) ppm; ^{13}C NMR (DMSO-d_6) δ: 160.49, 158.76, 154.70,

143.91, 131.65, 130.33, 127.39, 126.28, 114.31, 72.57, 55.29, 38.87, 31.33, 19.33, 13.59 ppm; Anal. calc. for $C_{17}H_{21}N_3O_4.1/3H_2O$: C, 60.52; H, 6.47; N, 12.46; found: C, 60.59; H, 6.822; N, 12.51%; HRMS calc. for $C_{17}H_{22}N_3O_4$ [M + H]: 332.1610, found: 332.1609.

4.1.5.13. [3-(4-Methoxyphenyl)-6-oxopyridazin-1(6H)-yl]methyl pentylcarbamate, 13a. Crystallized from ethanol/water to yield 57.2%; m.p. 67 °C; ^{1}H NMR (DMSO-d_6) δ: 8.07 (1H, d, *J:* 10 Hz, pyridazine H5), 7.84 (2H, d, *J:* 8.8 Hz, phenyl H2,6), 7.42 (1H, t, NH), 7.09–7.03 (3H, m, pyridazine H4, phenyl H3,5), 5.94 (2H, s, CH_2), 3.81 (3H, s, OCH_3), 2.98 (2H, q, CH_2), 1.41–1.37 (2H, m, CH_2), 1.26–1.21 (4H, m, CH_2), 0.83 (3H, t, CH_3) ppm; ^{13}C NMR (DMSO-d_6) δ: 160.49, 158.76, 154.69, 143.90, 131.64, 130.33, 127.38, 126.28, 114.30, 72.57, 55.29, 40.19, 28.88, 28.35, 21.75, 13.84 ppm; Anal. calc. for $C_{18}H_{23}N_3O_4.1/3H_2O$: C, 61.52; H, 6.79; N, 11.96; found: C, 61.59; H, 6.909; N, 11.91%; HRMS calc. for $C_{18}H_{24}N_3O_4$ [M + H]: 346.1767, found: 346.1774.

4.1.5.14. [3-(4-Methoxyphenyl)-6-oxopyridazin-1(6H)-yl]methyl hexylcarbamate, 14a. Crystallized from ethanol/water to yield 75.12%; m.p. 71 °C; ^{1}H NMR (DMSO-d_6) δ: 8.05 (1H, d, *J:* 9.6 Hz, pyridazine H5), 7.82 (2H, d, *J:* 8.8 Hz, phenyl H2,6), 7.40 (1H, t, NH), 7.07–7.02 (3H, m, pyridazine H4, phenyl H3,5), 5.92 (2H, s, CH_2), 3.79 (3H, s, OCH_3), 2.96 (2H, q, CH_2), 1.36–1.34 (2H, m, CH_2), 1.22–1.20 (6H, m, CH_2), 0.81 (3H, t, CH_3) ppm; ^{13}C NMR (DMSO-d_6) δ: 160.49, 158.77, 154.69, 143.89, 131.62, 130.32, 127.37, 126.28, 114.29, 72.54, 55.28, 40.23, 30.91, 29.17, 25.82, 21.99, 13.84 ppm; Anal. calc. for $C_{19}H_{25}N_3O_4.1/4H_2O$: C, 62.71; H, 7.06; N, 11.55; found: C, 62.88; H, 7.347; N, 11.61%; HRMS calc. for $C_{19}H_{26}N_3O_4$ [M + H]: 360.1923, found: 360.1921.

4.1.5.15. [3-(4-Methoxyphenyl)-6-oxopyridazin-1(6H)-yl]methyl cyclohexylcarbamate, 15a. Crystallized from ethanol/water to yield 50.9%; m.p. 144 °C; ^{1}H NMR (DMSO-d_6) δ: 8.04 (1H, d, *J:* 9.6 Hz, pyridazine H5), 7.81 (2H, d, *J:* 9.2 Hz, phenyl H2,6), 7.36 (1H, d, NH), 7.06–7.01 (3H, m, pyridazine H4, phenyl H3,5), 5.90 (2H, s, CH_2), 3.79 (3H, s, OCH_3), 3.26–3.24 (1H, m, cyclohexyl H1), 1.73–1.48 (5H, m, cyclohexyl equatorial), 1.22–1.05 (5H, m, cyclohexyl axial) ppm; ^{13}C NMR (DMSO-d_6) δ: 160.49, 158.77, 153.84, 143.90, 131.65, 130.32, 127.38, 126.27, 114.31, 72.57, 55.29, 49.48, 32.48, 25.07, 24.49 ppm; Anal. calc. for $C_{19}H_{23}N_3O_4$: C, 63.85; H, 6.49; N, 11.76; found: C, 63.85; H, 6.803; N, 11.67%; HRMS calc. for $C_{19}H_{24}N_3O_4$ [M + H]: 358.1767, found: 358.1763.

4.1.5.16. [3-(4-Methoxyphenyl)-6-oxopyridazin-1(6H)-yl]methyl heptylcarbamate, 16a. Crystallized from ethanol/water to yield 57.6%; m.p. 76 °C; ^{1}H NMR (DMSO-d_6) δ: 8.07 (1H, d, *J:* 10 Hz, pyridazine H5), 7.84 (2H, d, *J:* 8.8 Hz, phenyl H2,6), 7.41 (1H, t, NH), 7.08–7.03 (3H, m, pyridazine H4, phenyl H3,5), 5.94 (2H, s, CH_2), 3.81 (3H, s, OCH_3), 2.98 (2H, q, CH_2), 1.39–1.36 (2H, m, CH_2), 1.23–1.21 (8H, m, CH_2), 0.83 (3H, t, CH_3) ppm; ^{13}C NMR (DMSO-d_6) δ: 160.49, 158.76, 154.69, 143.89, 131.63, 130.33, 127.38, 126.29, 114.30, 72.52, 55.29, 40.22, 31.17, 29.20, 28.34, 26.11, 21.99, 3.89 ppm; Anal. calc. for $C_{20}H_{27}N_3O_4$: C, 64.32; H, 7.29; N, 11.25; found: C, 64.00; H, 7.673; N, 10.97%; HRMS calc. for $C_{20}H_{28}N_3O_4$ [M + H]: 374.2080, found: 374.2086.

4.1.5.17. [3-(4-Methoxyphenyl)-6-oxopyridazin-1(6H)-yl]methyl dimethylcarbamate, 17a. The crude product was purified by preparative TLC using dichloromethane-methanol (100:3) solvent system. Yield 13%; m.p. 120 °C; ^{1}H NMR (DMSO-d_6) δ: 8.05 (1H, d, *J:* 9.6 Hz, pyridazine H5), 7.82 (2H, d, *J:* 9.2 Hz, phenyl H2,6), 7.07–7.02 (3H, m, pyridazine H4, phenyl H3,5), 5.94 (2H, s, CH_2), 3.79 (3H, s, OCH_3), 2.82 (3H, s, CH_3), 2.78 (3H, s, CH_3) ppm; ^{13}C NMR (DMSO-d_6) δ: 160.49, 158.72, 154.24, 143.96, 131.73, 130.35, 127.42, 126.31, 114.33, 73.72, 55.29, 36.03, 35.53 ppm; Anal. calc. for $C_{15}H_{17}N_3O_4.1/2H_2O$: C, 57.68; H, 5.81; N, 13.45; found: C, 57.59; H, 5.530; N, 13.15%; HRMS calc. for $C_{15}H_{18}N_3O_4$ [M + H]: 304.1297, found: 304.1296.

4.1.5.18. 6-(3-Methoxyphenyl)pyridazin-3(2H)-one, 1b. Crystallized from water to yield 60%; m.p. 185 °C; HRMS calc. for $C_{11}H_{11}N_2O_2$ [M + H]: 203.0821, found: 203.0830 [30].

4.1.5.19. 2-(Hydroxymethyl)-6-(3-methoxyphenyl)pyridazin-3(2H)-one, 2b. The crude product was used without further purification due to the stability problem. Yield 78.7%; m.p. 133 °C; HRMS calc. for $C_{12}H_{13}N_2O_3$ [M + H]: 233.0926, found: 233.0935.

4.1.5.20. [3-(3-Methoxyphenyl)-6-oxopyridazin-1(6H)-yl] methylphenylcarbamate, 3b. Crystallized from acetonitrile to yield 68.6%; m.p. 198–201 °C; ^{1}H NMR (DMSO-d_6) δ: 9.92 (1H, s, NH), 8.10 (1H, d, *J:* 10 Hz, pyridazine H5), 7.46–7.36 (5H, m, phenyl H2,5,6, phenyl H2′,6′), 7.26 (2H, t, phenyl H3′,5′), 7.12 (1H, d, *J:* 10 Hz, pyridazine H4), 7.03–6.97 (2H, m, phenyl H4, phenyl H4′), 6.09 (2H, s, CH_2), 3.77 (3H, s, OCH_3) ppm; ^{13}C NMR (DMSO-d_6) δ: 159.69, 158.93, 151.98, 144.09, 138.58, 135.19, 132.10, 130.40, 130.11, 128.79, 122.78, 118.27, 115.40, 111.29, 72.91, 55.20 ppm; Anal. calc. for $C_{19}H_{17}N_3O_4$: C, 64.95; H, 4.88; N, 11.96, found: C, 64.74; H, 5.079; N, 12.06%; HRMS calc. for $C_{19}H_{18}N_3O_4$ [M + H]: 352.1297, found: 352.1295.

4.1.5.21. [3-(3-Methoxyphenyl)-6-oxopyridazin-1(6H)-yl]methyl (4-fluorophenyl)carbamate, 4b. Crystallized from acetonitrile to yield 80.2%; m.p. 192–193 °C; ^{1}H NMR (DMSO-d_6) δ: 9.97 (1H, s, NH), 8.11 (1H, d, *J:* 10 Hz, pyridazine H5), 7.46–7.37 (5H, m, phenyl H2,5,6, phenyl H2′,6′), 7.13–7.09 (3H, m, phenyl H3′,5′, pyridazine H4), 7.03 (1H, dd, J_1: 7.8 Hz, J_2: 2.4 Hz, phenyl H4), 6.08 (2H, s, CH_2), 3.77 (3H, s, OCH_3) ppm; ^{13}C NMR (DMSO-d_6) δ: 159.70, 158.94, 157.83 (d, *J:* 239.38 Hz, F-phenyl H4′), 152.10, 144.11, 135.19, 134.95, 132.12, 130.41, 130.11, 119.99, 118.28, 115.40 (d, *J:* 22.64 Hz, F-phenyl H3′, 5′), 115.38, 111.32, 72.98, 55.21 ppm; Anal. calc. for $C_{19}H_{16}FN_3O_4$: C, 61.79; H, 4.37; N, 11.38, found: C, 61.43; H, 4.494; N, 11.40%; HRMS calc. for $C_{19}H_{17}FN_3O_4$ [M + H]: 370.1203, found: 370.1194.

4.1.5.22. [3-(3-Methoxyphenyl)-6-oxopyridazin-1(6H)-yl]methyl (4-chlorophenyl)carbamate, 5b. Crystallized from acetonitrile to yield 76.6%; m.p. 194–195 °C; ^{1}H NMR (DMSO-d_6) δ: 10.08 (1H, s, NH), 8.11 (1H, d, *J:* 10 Hz, pyridazine H5), 7.47–7.37 (5H, m, phenyl H2,5,6, phenyl H2′,6′), 7.32 (2H, d, *J:* 9.2 Hz, phenyl H3′,5′), 7.11 (1H, d, *J:* 10 Hz, pyridazine H4), 7.03 (1H, dd, J_1: 8.2 Hz, J_2: 2.4 Hz, phenyl H4), 6.09 (2H, s, CH_2), 3.77 (3H, s, OCH_3) ppm; ^{13}C NMR (DMSO-d_6) δ: 159.69, 158.93, 151.94, 144.12, 137.62, 135.17, 132.13, 130.41, 130.11, 128.72, 126.45, 119.75, 118.27, 115.38, 111.32, 73.06, 55.21 ppm; Anal. calc. for $C_{19}H_{16}ClN_3O_4$: C, 59.15; H, 4.18; N, 10.89, found: C, 58.88; H, 4.286; N, 10.95%; HRMS calc. for $C_{19}H_{17}ClN_3O_4$ [M + H]: 386.0908, found: 386.0891.

4.1.5.23. [3-(3-Methoxyphenyl)-6-oxopyridazin-1(6H)-yl]methyl (4-methoxyphenyl)carbamate, 6b. Crystallized from acetonitrile to yield 56.1%; m.p. 183 °C; ^{1}H NMR (DMSO-d_6) δ: 9.73 (1H, s, NH), 8.10 (1H, d, *J:* 10 Hz, pyridazine H5), 7.46–7.33 (5H, m, phenyl H2,5,6, phenyl H2′,6′), 7.11 (1H, d, *J:* 10 Hz, pyridazine H4), 7.04–7.01 (1H, m, phenyl H4), 6.84 (2H, d, *J:* 8.8 Hz, phenyl H3′,5′), 6.06 (2H, s, CH_2), 3.77 (3H, s, OCH_3), 3.68 (3H, s, OCH_3) ppm; ^{13}C NMR (DMSO-d_6) δ: 159.69, 158.93, 155.01, 152.11, 144.05, 135.21, 132.08, 131.58, 130.40, 130.11, 119.86, 118.27, 115.38, 113.99, 111.30, 72.84, 55.21, 55.14 ppm; Anal. calc. for $C_{20}H_{19}N_3O_5$: C, 62.99; H, 5.02; N, 11.02, found: C, 62.96; H, 5.232; N, 10.99%; HRMS calc. for $C_{20}H_{20}N_3O_5$ [M + H]: 382.1403, found: 382.1400.

4.1.5.24. [3-(3-Methoxyphenyl)-6-oxopyridazin-1(6H)-yl]methyl (4-methylphenyl)carbamate, 7b. Crystallized from acetonitrile to yield

67.2%; m.p. 191 °C; ^{1}H NMR (DMSO-d_6) δ: 9.83 (1H, s, NH), 8.14 (1H, d, *J:* 10 Hz, pyridazine H5), 7.46–7.39 (3H, m, phenyl H2,5,6), 7.34 (2H, d, *J:* 8 Hz, phenyl H2′,6′), 7.14 (1H, d, *J:* 9.6 Hz, pyridazine H4), 7.09 (2H, d, *J:* 8 Hz, phenyl H3′,5′), 7.06–7.04 (1H, dd, J_1*:* 7.8 Hz, J_2*:* 2.8 Hz, phenyl H4), 6.09 (2H, s, CH_2), 3.79 (3H, s, OCH_3), 2.23 (3H, s, CH_3) ppm; ^{13}C NMR (DMSO-d_6) δ: 159.68, 158.92, 151.98, 144.06, 136.02, 135.20, 132.07, 131.65, 130.39, 130.10, 129.16, 118.26, 115.38, 111.29, 72.86, 55.20, 20.30 ppm; Anal. calc. for $C_{20}H_{19}N_3O_4$: C, 65.74; H, 5.24; N, 11.50, found: C, 65.60; H, 5.406; N, 11.57%; HRMS calc. for $C_{20}H_{20}N_3O_4$ [M + H]: 366.1454, found: 366.1452.

4.1.5.25. [3-(3-Methoxyphenyl)-6-oxopyridazin-1(6H)-yl]methyl methylcarbamate, 8b. Crystallized from acetone/water to yield 38.8%; m.p. 114 °C; ^{1}H NMR (DMSO-d_6) δ: 8.09 (1H, d, *J:* 9.6 Hz, pyridazine H5), 7.46–7.38 (3H, m, phenyl H2,5,6), 7.29 (1H, q, NH), 7.09 (1H, d, *J:* 10 Hz, pyridazine H4), 7.05–7.02 (1H, m, phenyl H4), 5.94 (2H, s, CH_2), 3.80 (3H, s, OCH_3), 2.57 (3H, d, N-CH_3) ppm; ^{13}C NMR (DMSO-d_6) δ: 159.69, 158.86, 155.19, 143.88, 135.27, 131.95, 130.35, 130.10, 118.25, 115.27, 111.36, 72.76, 55.24, 26.89 ppm; Anal. calc. for $C_{14}H_{15}N_3O_4$: C, 58.13; H, 5.23; N, 14.53, found: C, 58.18; H, 5.370; N, 14.50%; HRMS calc. for $C_{14}H_{16}N_3O_4$ [M + H]: 290.1141, found: 290.1154.

4.1.5.26. [3-(3-Methoxyphenyl)-6-oxopyridazin-1(6H)-yl]methyl ethylcarbamate, 9b. Crystallized from ethanol/water to yield 72.5%; m.p. 112 °C; ^{1}H NMR (DMSO-d_6) δ: 8.11 (1H, d, *J:* 10.4 Hz, pyridazine H5), 7.47–7.39 (4H, m, phenyl H2,5,6, NH), 7.10 (1H, d, *J:* 9.6 Hz, pyridazine H4), 7.06–7.04 (1H, m, phenyl H4), 5.97 (2H, s, CH_2), 3.82 (3H, s, OCH_3), 3.07–3.00 (2H, m, CH_2), 1.01 (3H, t, CH_3) ppm; ^{13}C NMR (DMSO-d_6) δ: 159.69, 158.87, 154.49, 143.89, 135.27, 131.94, 130.35, 130.10, 118.25, 115.27, 111.37, 72.63, 55.24, 35.08, 14.82 ppm; Anal. calc. for $C_{15}H_{17}N_3O_4$: C, 59.40; H, 5.65; N, 13.85, found: C, 59.49; H, 5.446; N, 13.83%; HRMS calc. for $C_{20}H_{20}N_3O_5$ [M + H]: 382.1403, found: 382.1400.

4.1.5.27. [3-(3-Methoxyphenyl)-6-oxopyridazin-1(6H)-yl]methyl propylcarbamate, 10b. Crystallized from ethanol/water to yield 80.9%; m.p. 101 °C; ^{1}H NMR (DMSO-d_6) δ: 8.11 (1H, d, *J:* 10.4 Hz, pyridazine H5), 7.48–7.40 (4H, m, phenyl H2,5,6, NH), 7.11 (1H, d, *J:* 9.6 Hz, pyridazine H4), 7.07–7.04 (1H, m, phenyl H4), 5.96 (2H, s, CH_2), 3.82 (3H, s, OCH_3), 2.96 (2H, q, CH_2), 1.43–1.38 (2H, m, CH_2), 0.82 (3H, t, CH_3) ppm; ^{13}C NMR (DMSO-d_6) δ: 159.69, 158.87, 154.70, 143.88, 135.26, 131.94, 130.35, 130.09, 118.25, 115.26, 111.37, 72.62, 55.24, 42.03, 22.47, 11.15 ppm; Anal. calc. for $C_{16}H_{19}N_3O_4$: C, 60.56; H, 6.03; N, 13.24, found: C, 60.68; H, 6.242; N, 13.14%; HRMS calc. for $C_{16}H_{20}N_3O_4$ [M + H]: 318.1454, found: 318.1458.

4.1.5.28. [3-(3-Methoxyphenyl)-6-oxopyridazin-1(6H)-yl]methyl propan-2-ylcarbamate, 11b. Crystallized from ethanol/water to yield 74.5%; m.p. 126 °C; ^{1}H NMR (DMSO-d_6) δ: 8.11 (1H, d, *J:* 10 Hz, pyridazine H5), 7.48–7.37 (4H, m, phenyl H2,5,6, NH), 7.11 (1H, d, *J:* 9.6 Hz, pyridazine H4), 7.07–7.04 (1H, m, phenyl H4), 5.95 (2H, s, CH_2), 3.82 (3H, s, OCH_3), 3.62–3.59 (1H, m, CH), 1.05 (6H, d, CH_3) ppm; ^{13}C NMR (DMSO-d_6) δ: 159.69, 158.86, 153.78, 143.87, 135.26, 131.92, 130.33, 130.08, 118.24, 115.25, 111.37, 72.53, 55.24, 42.41, 22.37 ppm; Anal. calc. for $C_{16}H_{19}N_3O_4$: C, 60.56; H, 6.03; N, 13.24, found: C, 60.52; H, 6.271; N, 13.16%; HRMS calc. for $C_{16}H_{20}N_3O_4$ [M + H]: 318.1454, found: 318.1456.

4.1.5.29. [3-(3-Methoxyphenyl)-6-oxopyridazin-1(6H)-yl]methyl butylcarbamate, 12b. Crystallized from ethanol/water to yield 59.9%; m.p. 84 °C; ^{1}H NMR (DMSO-d_6) δ: 8.09 (1H, d, *J:* 9.6 Hz, pyridazine H5), 7.45–7.38 (4H, m, phenyl H2,5,6, NH), 7.08 (1H, d, *J:* 9.6 Hz, pyridazine H4), 7.05–7.02 (1H, m, phenyl H4), 5.94 (2H, s, CH_2), 3.80 (3H, s, OCH_3), 2.97 (2H, q, CH_2), 1.37–1.31 (2H, m, CH_2), 1.26–1.20 (2H, m, CH_2), 0.82 (3H, t, CH_3) ppm; ^{13}C NMR (DMSO-d_6) δ: 159.67, 158.85, 154.66, 143.86, 135.25, 131.91, 130.33, 130.07, 118.22, 115.23, 111.36, 72.56, 55.21, 39.90, 31.31, 19.32, 13.56 ppm; Anal. calc. for $C_{17}H_{21}N_3O_4$: C, 61.62; H, 6.39; N, 12.68, found: C, 61.55; H, 6.626; N, 12.68%; HRMS calc. for $C_{17}H_{22}N_3O_4$ [M + H]: 332.1610, found: 332.1601.

4.1.5.30. [3-(3-Methoxyphenyl)-6-oxopyridazin-1(6H)-yl]methyl pentylcarbamate, 13b. Crystallized from ethanol/water to yield 81.9%; m.p. 99 °C; ^{1}H NMR (DMSO-d_6) δ: 8.11 (1H, d, *J:* 10.4 Hz, pyridazine H5), 7.47–7.39 (4H, m, phenyl H2,5,6, NH), 7.10 (1H, d, *J:* 9.6 Hz, pyridazine H4), 7.07–7.04 (1H, m, phenyl H4), 5.96 (2H, s, CH_2), 3.82 (3H, s, OCH_3), 2.98 (2H, q, CH_2), 1.40–1.35 (2H, m, CH_2), 1.27–1.19 (4H, m, CH_2), 0.83 (3H, t, CH_3) ppm; ^{13}C NMR (DMSO-d_6) δ: 159.68, 158.86, 154.65, 143.86, 135.25, 131.91, 130.33, 130.06, 118.22, 115.22, 111.37, 72.55, 55.22, 40.20, 28.86, 28.34, 21.73, 13.82 ppm; Anal. calc. for $C_{18}H_{23}N_3O_4$: C, 62.59; H, 6.71; N, 12.17, found: C, 62.31; H, 6.960; N, 12.08%; HRMS calc. for $C_{18}H_{24}N_3O_4$ [M + H]: 346.1767, found: 346.1767.

4.1.5.31. [3-(3-Methoxyphenyl)-6-oxopyridazin-1(6H)-yl]methyl hexylcarbamate, 14b. Crystallized from ethanol/water to yield 73.7%; m.p. 85 °C; ^{1}H NMR (DMSO-d_6) δ: 8.08 (1H, d, *J:* 9.6 Hz, pyridazine H5), 7.45–7.37 (4H, m, phenyl H2,5,6, NH), 7.08 (1H, d, *J:* 10 Hz, pyridazine H4), 7.04–7.01 (1H, m, phenyl H4), 5.93 (2H, s, CH_2), 3.79 (3H, s, OCH_3), 2.95 (2H, q, CH_2), 1.37–1.32 (2H, m, CH_2), 1.23–1.19 (6H, m, CH_2), 0.80 (3H, t, CH_3) ppm; ^{13}C NMR (DMSO-d_6) δ: 159.68, 158.85, 154.65, 143.85, 135.25, 131.90, 130.33, 130.06, 118.22, 115.22, 111.37, 72.54, 55.22, 40.23, 30.88, 29.15, 25.81, 21.97, 13.83 ppm; Anal. calc. for $C_{19}H_{25}N_3O_4$: C, 63.49; H, 7.01; N, 11.69, found: C, 63.69; H, 7.076; N, 11.62%; HRMS calc. for $C_{19}H_{26}N_3O_4$ [M + H]: 360.1923, found: 360.1919.

4.1.5.32. [3-(3-Methoxyphenyl)-6-oxopyridazin-1(6H)-yl]methyl cyclohexylcarbamate, 15b. Crystallized from acetonitrile/water to yield 67.5%; m.p. 148 °C; ^{1}H NMR (DMSO-d_6) δ: 8.08 (1H, d, *J:* 9.6 Hz, pyridazine H5), 7.45–7.37 (4H, m, phenyl H2,5,6, NH), 7.08 (1H, d, *J:* 10 Hz, pyridazine H4), 7.04–7.01 (1H, m, phenyl H4), 5.93 (2H, s, CH_2), 3.79 (3H, s, OCH_3), 3.26–3.24 (1H, m, cyclohexyl H1), 1.73–1.48 (5H, m, cyclohexyl equatorial), 1.22–1.01 (5H, m, cyclohexyl axial) ppm; ^{13}C NMR (DMSO-d_6) δ: 159.69, 158.87, 153.82, 143.86, 135.25, 131.92, 130.33, 130.08, 118.23, 115.23, 111.39, 72.52, 55.23, 49.51, 32.48, 25.07, 24.49 ppm; Anal. calc. for $C_{19}H_{23}N_3O_4$: C, 63.85; H, 6.49; N, 11.76, found: C, 63.91; H, 6.834; N, 11.71%; HRMS calc. for $C_{19}H_{24}N_3O_4$ [M + H]: 358.1767, found: 358.1765.

4.1.5.33. [3-(3-Methoxyphenyl)-6-oxopyridazin-1(6H)-yl]methyl heptylcarbamate, 16b. Crystallized from ethanol/water to yield 64.3%; m.p. 96 °C; ^{1}H NMR (DMSO-d_6) δ: 8.09 (1H, d, *J:* 9.6 Hz, pyridazine H5), 7.45–7.37 (4H, m, phenyl H2,5,6, NH), 7.08 (1H, d, *J:* 10 Hz, pyridazine H4), 7.04–7.02 (1H, m, phenyl H4), 5.93 (2H, s, CH_2), 3.79 (3H, s, OCH_3), 2.95 (2H, q, CH_2), 1.37–1.33 (2H, m, CH_2), 1.24–1.18 (8H, m, CH_2), 0.81 (3H, t, CH_3) ppm; ^{13}C NMR (DMSO-d_6) δ: 159.69, 158.86, 154.65, 143.85, 135.26, 131.91, 130.33, 130.06, 118.22, 115.23, 111.37, 72.53, 55.22, 40.23, 31.15, 29.19, 28.31, 26.10, 21.98, 13.88 ppm; Anal. calc. for $C_{20}H_{27}N_3O_4$: C, 64.32; H, 7.29; N, 11.25, found: C, 64.27; H, 7.547; N, 11.12%; HRMS calc. for $C_{20}H_{28}N_3O_4$ [M + H]: 374.2080, found: 374.2067.

4.1.5.34. [3-(3-Methoxyphenyl)-6-oxopyridazin-1(6H)-yl]methyl dimethylcarbamate, 17b. Crystallized from water to yield 28.2%; m.p. 95 °C; ^{1}H NMR (DMSO-d_6) δ: 8.10 (1H, d, *J:* 9.6 Hz, pyridazine H5), 7.46–7.38 (3H, m, phenyl H2,5,6), 7.09 (1H, d, *J:* 9.6 Hz, pyridazine H4), 7.05–7.03 (1H, m, phenyl H4), 5.96 (2H, s, CH_2), 3.80 (3H, s, OCH_3), 2.82 (3H, s, CH_3), 2.79 (3H, s, CH_3) ppm; ^{13}C NMR (DMSO-d_6) δ: 159.68, 158.81, 154.22, 143.92, 135.30, 132.00, 130.36, 130.10, 118.28, 115.27, 111.39, 73.70, 55.24, 36.04, 35.53, ppm; Anal. calc.

for $C_{15}H_{17}N_3O_4$: C, 59.40; H, 5.65; N, 13.85, found: C, 59.14; H, 6.001; N, 13.97%; HRMS calc. for $C_{15}H_{18}N_3O_4$ [M + H]: 304.1297, found: 304.1306.

4.1.5.35. 6-(2-Methoxyphenyl)pyridazin-3(2H)-one, 1c. Crystallized from ethanol/water to yield 72.4%; m.p. 170 °C; HRMS calc. for $C_{11}H_{11}N_2O_2$ [M + H]: 203.0821, found: 203.0821 [30].

4.1.5.36. 2-(Hydroxymethyl)-6-(2-methoxyphenyl)pyridazin-3(2H)-one, 2c. The crude product was used without further purification due to the stability problem. Yield 90%; m.p. 143–144 °C; HRMS calc. for $C_{12}H_{13}N_2O_3$ [M + H]: 233.0926, found: 233.0935.

4.1.5.37. [3-(2-Methoxyphenyl)-6-oxopyridazin-1(6H)-yl]methyl phenylcarbamate, 3c. Crystallized from ethanol/water to yield 70.2%; m.p. 155 °C; ^{1}H NMR (DMSO-d_6) δ: 9.90 (1H, s, NH), 7.75 (1H, d, *J:* 9.6 Hz, pyridazine H5), 7.46–7.43 (4H, m, phenyl H4,6, phenyl H2′,6′), 7.26 (2H, t, *J:* 8 Hz, phenyl H3′,5′), 7.14 (1H, d, *J:* 8.8 Hz, phenyl H3), 7.05–6.97 (3H, m, pyridazine H4, phenyl H5, phenyl H4′), 6.05 (2H, s, CH_2), 3.80 (3H, s, OCH_3) ppm; ^{13}C NMR (DMSO-d_6) δ: 158.97, 156.82, 151.97, 144.77, 138.60, 135.78, 131.31, 129.68, 128.79, 128.67, 123.62, 122.76, 120.77, 118.26, 111.96, 72.95, 55.73 ppm; Anal. calc. for $C_{19}H_{17}N_3O_4$: C, 64.95; H, 4.88; N, 11.96, found: C, 65.03; H, 5.130; N, 11.89%; HRMS calc. for $C_{19}H_{18}N_3O_4$ [M + H]: 352.1297, found: 352.1297.

4.1.5.38. [3-(2-Methoxyphenyl)-6-oxopyridazin-1(6H)-yl]methyl (4-fluorophenyl)carbamate, 4c. Crystallized from ethanol/water to yield 45.6%; m.p. 158 °C; ^{1}H NMR (DMSO-d_6) δ: 9.95 (1H, s, NH), 7.75 (1H, d, *J:* 9.6 Hz, pyridazine H5), 7.47–7.42 (4H, m, phenyl H4,6, phenyl H2′,6′), 7.15–7.00 (5H, m, pyridazine H4, phenyl H3,5, phenyl H3′,5′), 6.04 (2H, s, CH_2), 3.80 (3H, s, OCH_3) ppm; ^{13}C NMR (DMSO-d_6) δ: 158.97, 157.8 (d, *J:* 234.7 Hz, F-phenyl H4′), 156.82, 152.08, 144.78, 135.78, 134.94, 131.31, 129.67, 128.67, 123.61, 120.77, 119.91, 115.39 (d, *J:* 22.4 Hz, F-phenyl H3′,5′), 111.96, 73.00, 55.72 ppm; Anal. calc. for $C_{19}H_{16}FN_3O_4$: C, 61.79; H, 4.37; N, 11.38, found: C, 61.65; H, 4.475; N, 11.47%; HRMS calc. for $C_{19}H_{17}FN_3O_4$ [M + H]: 370.1203, found: 370.1188.

4.1.5.39. [3-(2-Methoxyphenyl)-6-oxopyridazin-1(6H)-yl]methyl (4-chlorophenyl)carbamate, 5c. Crystallized from ethanol/water to yield 41.5%; m.p. 162 °C; ^{1}H NMR (DMSO-d_6) δ: 10.06 (1H, s, NH), 7.75 (1H, d, *J:* 9.6 Hz, pyridazine H5), 7.47–7.43 (4H, m, phenyl H4,6, phenyl H2′,6′), 7.34–7.31 (2H, m, phenyl H3′,5′), 7.15 (1H, d, *J:* 8.4 Hz, phenyl H3), 7.05–7.00 (2H, m, pyridazine H4, phenyl H5), 6.05 (2H, s, CH_2), 3.80 (3H, s, OCH_3) ppm; ^{13}C NMR (DMSO-d_6) δ: 158.89, 156.74, 151.85, 144.72, 137.54, 135.73, 131.25, 129.59, 128.64, 128.60, 126.35, 123.52, 120.69, 119.66, 111.89, 72.99, 55.66 ppm; Anal. calc. for $C_{19}H_{16}ClN_3O_4$: C, 59.15; H, 4.18; N, 10.89, found: C, 59.21; H, 4.125; N, 10.82%; HRMS calc. for $C_{19}H_{17}ClN_3O_4$ [M + H]: 386.0908, found: 386.0896.

4.1.5.40. [3-(2-Methoxyphenyl)-6-oxopyridazin-1(6H)-yl]methyl (4-methoxyphenyl)carbamate, 6c. Crystallized from ethanol/water to yield 16.3%; m.p. 157 °C; ^{1}H NMR (DMSO-d_6) δ: 9.71 (1H, s, NH), 7.75 (1H, d, *J:* 9.6 Hz, pyridazine H5), 7.47–7.42 (2H, m, phenyl H4,6), 7.33 (2H, d, *J:* 8.8 Hz, phenyl H2′,6′), 7.14 (1H, d, *J:* 8.8 Hz, phenyl H3), 7.05–6.99 (2H, m, phenyl H5, pyridazine H4), 6.84 (2H, d, *J:* 8.8 Hz, phenyl H3′,5′), 6.02 (2H, s, CH_2), 3.80 (3H, s, OCH_3), 3.67 (3H, s, OCH_3) ppm; ^{13}C NMR (DMSO-d_6) δ: 158.97, 156.82, 154.99, 152.10, 144.72, 135.74, 131.59, 131.30, 129.68, 128.67, 123.63, 120.77, 119.84, 113.99, 111.96, 72.87, 55.73, 55.14 ppm; Anal. calc. for $C_{20}H_{19}N_3O_5$: C, 62.99; H, 5.02; N, 11.02, found: C, 62.82; H, 5.116; N, 11.02%; HRMS calc. for $C_{20}H_{20}N_3O_5$ [M + H]: 382.1403, found: 382.1404.

4.1.5.41. [3-(2-Methoxyphenyl)-6-oxopyridazin-1(6H)-yl]methyl (4-methylphenyl)carbamate, 7c. Crystallized from ethanol/water to yield 60%; m.p. 144 °C; ^{1}H NMR (DMSO-d_6) δ: 9.79 (1H, s, NH), 7.76 (1H, d, *J:* 9.6 Hz, pyridazine H5), 7.47–7.43 (2H, m, phenyl H4,6), 7.31 (2H, d, *J:* 8.8 Hz, phenyl H2′,6′), 7.15 (1H, d, *J:* 8.8 Hz, phenyl H3), 7.07–7.00 (4H, m, phenyl H3′,5′,5, pyridazine H4), 6.03 (2H, s, CH_2), 3.81 (3H, s, OCH_3), 2.21 (3H, s, CH_3) ppm; ^{13}C NMR (DMSO-d_6) δ: 158.96, 156.81, 151.97, 144.74, 136.03, 135.75, 131.63, 131.30, 129.67, 129.17, 128.66, 123.62, 120.77, 118.28, 111.96, 72.89, 55.72, 20.30 ppm; Anal. calc. for $C_{20}H_{19}N_3O_4$: C, 65.74; H, 5.24; N, 11.50, found: C, 65.97; H, 5.185; N, 11.49%; HRMS calc. for $C_{20}H_{20}N_3O_4$ [M + H]: 366.1454, found: 366.1452.

4.1.5.42. [3-(2-Methoxyphenyl)-6-oxopyridazin-1(6H)-yl]methyl methylcarbamate, 8c. Crystallized from acetone/water to yield 37.8%; m.p. 149 °C; ^{1}H NMR (DMSO-d_6) δ: 7.73 (1H, d, *J:* 10 Hz, pyridazine H5), 7.47–7.42 (2H, m, phenyl H4,6), 7.27 (1H, q, NH), 7.15 (1H, d, *J:* 8.8 Hz, phenyl H3), 7.04 (1H, t, *J:* 7.2 Hz, phenyl H5), 6.98 (1H, d, *J:* 9,6 Hz, pyridazine H4), 5.90 (2H, s, CH_2), 3.81 (3H, s, OCH_3), 2.55 (3H, d, CH_3) ppm; ^{13}C NMR (DMSO-d_6) δ: 158.89, 156.80, 155.18, 144.52 135.60, 131.25, 129.68, 128.61, 123.66, 120.76, 111.94, 72.73, 55.71, 26.87 ppm; Anal. calc. for $C_{14}H_{15}N_3O_4$: C, 58.13; H, 5.23; N, 14.53, found: C, 57.90; H, 5.283; N, 14.46%; HRMS calc. for $C_{14}H_{16}N_3O_4$ [M + H]: 290.1141, found: 290.1142.

4.1.5.43. [3-(2-Methoxyphenyl)-6-oxopyridazin-1(6H)-yl]methyl ethylcarbamate, 9c. Crystallized from ethanol/water to yield 48%; m.p. 116 °C; ^{1}H NMR (DMSO-d_6) δ: 7.73 (1H, d, *J:* 10 Hz, pyridazine H5), 7.47–7.39 (3H, m, NH, phenyl H4,6), 7.15 (1H, d, *J:* 8 Hz, phenyl H3), 7.04 (1H, t, *J:* 7.6 Hz, phenyl H5), 6.98 (1H, d, *J:* 9.6 Hz, pyridazine H4), 5.90 (2H, s, CH_2), 3.81 (3H, s, OCH_3), 3.03–2.96 (2H, m, CH_2), 0.98 (3H, t, CH_3) ppm; ^{13}C NMR (DMSO-d_6) δ: 158.91, 156.81, 154.49, 144.53, 135.60, 131.26, 129.68, 128.61, 123.67, 120.75, 111.95, 72.62, 55.72, 35.06, 14.82 ppm; Anal. calc. for $C_{15}H_{17}N_3O_4$: C, 59.40; H, 5.65; N, 13.85, found: C, 59.48; H, 5.724; N, 13.81%; HRMS calc. for $C_{15}H_{18}N_3O_4$ [M + H]: 304.1297, found: 304.1296.

4.1.5.44. [3-(2-Methoxyphenyl)-6-oxopyridazin-1(6H)-yl]methyl propylcarbamate, 10c. Crystallized from acetone/water to yield 31.8%; m.p. 146 °C; ^{1}H NMR (DMSO-d_6) δ: 7.73 (1H, d, *J:* 9.6 Hz, pyridazine H5), 7.47–7.40 (3H, m, NH, phenyl H4,6), 7.15 (1H, d, *J:* 8.4 Hz, phenyl H3), 7.04 (1H, td, J_1: 7.6 Hz, J_2: 1.2 Hz, phenyl H5), 6.98 (1H, d, *J:* 9.6 Hz, pyridazine H4), 5.90 (2H, s, CH_2), 3.81 (3H, s, OCH_3), 2.92 (2H, q, CH_2), 1.40–1.35 (2H, m, CH_2), 0.79 (3H, t, CH_3) ppm; ^{13}C NMR (DMSO-d_6) δ: 158.89, 156.80, 154.68, 144.51, 135.58, 131.25, 129.66, 128.60, 123.66, 120.73, 111.94, 72.60, 55.71, 42.01, 22.45, 11.13 ppm; Anal. calc. for $C_{16}H_{19}N_3O_4$: C, 60.56; H, 6.03; N, 13.24, found: C, 60.74; H, 6.180; N, 13.26%; HRMS calc. for $C_{16}H_{20}N_3O_4$ [M + H]: 318.1454, found: 318.1441.

4.1.5.45. [3-(2-Methoxyphenyl)-6-oxopyridazin-1(6H)-yl]methyl propan-2-ylcarbamate, 11c. Crystallized from ethanol/water to yield 64.1%; m.p. 115 °C; ^{1}H NMR (DMSO-d_6) δ: 7.73 (1H, d, *J:* 10 Hz, pyridazine H5), 7.47–7.42 (2H, m, phenyl H4,6), 7.34 (1H, d, NH), 7.15 (1H, d, *J:* 8.4 Hz, phenyl H3), 7.04 (1H, td, J_1: 7.6 Hz, J_2: 1.2 Hz, phenyl H5), 6.98 (1H, d, *J:* 9.6 Hz, pyridazine H4), 5.90 (2H, s, CH_2), 3.81 (3H, s, OCH_3), 3.60–3.55 (1H, m, CH), 1.02 (6H, d, CH_3) ppm; ^{13}C NMR (DMSO-d_6) δ: 158.89, 156.79, 153.76, 144.50, 135.56, 131.23, 129.64, 128.58, 123.64, 120.72, 111.93, 72.50, 55.70, 42.36, 22.35 ppm. Anal. calc. for $C_{16}H_{19}N_3O_4$: C, 60.56; H, 6.03; N, 13.24, found: C, 60.51; H, 6.115; N, 13.18%; HRMS calc. for $C_{16}H_{20}N_3O_4$ [M + H]: 318.1454, found: 318.1441.

4.1.5.46. [3-(2-Methoxyphenyl)-6-oxopyridazin-1(6H)-yl]methyl butylcarbamate, 12c. Crystallized from ethanol/water to yield 58%; m.p. 95 °C; ^{1}H NMR (DMSO-d_6) δ: 7.73 (1H, d, *J:* 10 Hz, pyridazine H5),

7.47–7.38 (3H, m, NH, phenyl H4,6), 7.15 (1H, d, *J*: 8 Hz, phenyl H3), 7.04 (1H, td, J_1: 7.2 Hz, J_2: 0.8 Hz, phenyl H5), 6.98 (1H, d, *J*: 9.6 Hz, pyridazine H4), 5.90 (2H, s, CH_2), 3.81 (3H, s, OCH_3), 2.96 (2H, q, CH_2), 1.36–1.31 (2H, m, CH_2), 1.26–1.20 (2H, m, CH_2), 0.82 (3H, t, CH_3) ppm; ^{13}C NMR (DMSO-d_6) δ: 158.90, 156.81, 154.67, 144.51, 135.57, 131.24, 129.66, 128.59, 123.67, 120.73, 111.94, 72.57, 55.70, 39.91, 31.30, 19.32, 13.56 ppm. Anal. calc. for $C_{17}H_{21}N_3O_4$: C, 61.62; H, 6.39; N, 12.68, found: C, 61.70; H, 6.630; N, 12.75%; HRMS calc. for $C_{17}H_{22}N_3O_4$ [M + H]: 332.1610, found: 332.1610.

4.1.5.47. [3-(2-Methoxyphenyl)-6-oxopyridazin-1(6H)-yl]methyl pentylcarbamate, 13c. Crystallized from ethanol/water to yield 88.3%; m.p. 100 °C; ^{1}H NMR (DMSO-d_6) δ: 7.73 (1H, d, *J*: 10 Hz, pyridazine H5), 7.47–7.38 (3H, m, NH, phenyl H4,6), 7.15 (1H, d, *J*: 8.4 Hz, phenyl H3), 7.03 (1H, td, J_1: 7.2, J_2: 0.8 Hz, phenyl H5), 6.98 (1H, d, *J*: 9.6 Hz, pyridazine H4), 5.90 (2H, s, CH_2), 3.81 (3H, s, OCH_3), 2.95 (2H, q, CH_2), 1.38–1.33 (2H, m, CH_2), 1.24–1.17 (4H, m, CH_2), 0.81 (3H, t, CH_3) ppm; ^{13}C NMR (DMSO-d_6) δ: 158.90, 156.81, 154.66, 144.51, 135.57, 131.24, 129.66, 128.60, 123.66, 120.72, 111.94, 72.57, 55.70, 40.18, 28.86, 28.35, 21.75, 13.84 ppm; Anal. calc. for $C_{18}H_{23}N_3O_4$: C, 62.59; H, 6.71; N, 12.17, found: C, 62.88; H, 6.795; N, 12.21%; HRMS calc. for $C_{18}H_{24}N_3O_4$ [M + H]: 346.1767, found: 346.1756.

4.1.5.48. [3-(2-Methoxyphenyl)-6-oxopyridazin-1(6H)-yl]methyl hexylcarbamate, 14c. Crystallized from ethanol/water to yield 80.6%; m.p. 89 °C; ^{1}H NMR (DMSO-d_6) δ: 7.73 (1H, d, *J*: 9.6 Hz, pyridazine H5), 7.47–7.38 (3H, m, NH, phenyl H4,6), 7.14 (1H, d, *J*: 8 Hz, phenyl H3), 7.03 (1H, t, *J*: 7.2 Hz, phenyl H5), 6.97 (1H, d, *J*: 9.6 Hz, pyridazine H4), 5.90 (2H, s, CH_2), 3.80 (3H, s, OCH_3), 2.94 (2H, q, CH_2), 1.36–1.31 (2H, m, CH_2), 1.22–1.19 (6H, m, CH_2), 0.81 (3H, t, CH_3) ppm; ^{13}C NMR (DMSO-d_6) δ: 158.83, 156.74, 154.59, 144.44, 135.50, 131.18, 129.59, 128.53, 123.60, 120.65, 111.88, 72.49, 55.64, 40.14, 30.82, 29.07, 25.74, 21.91, 13.77 ppm; Anal. calc. for $C_{19}H_{25}N_3O_4$: C, 63.49; H, 7.01; N, 11.69, found: C, 63.93; H, 6.938; N, 11.64%; HRMS calc. for $C_{19}H_{26}N_3O_4$ [M + H]: 360.1923, found: 360.1915.

4.1.5.49. [3-(2-Methoxyphenyl)-6-oxopyridazin-1(6H)-yl]methyl cyclohexylcarbamate, 15c. Crystallized from acetone/water to yield 47.7%; m.p. 168 °C; ^{1}H NMR (DMSO-d_6) δ: 7.75 (1H, d, *J:* 9.6 Hz, pyridazine H5), 7.49–7.45 (2H, m, phenyl H4,6), 7.39 (1H, d, NH), 7.17 (1H, d, *J*: 8 Hz, phenyl H3), 7.06 (1H, t, *J*: 7.2 Hz, phenyl H5), 7.00 (1H, d, *J*: 9.6 Hz, pyridazine H4), 5.92 (2H, s, CH_2), 3.83 (3H, s, OCH_3), 3.27–3.25 (1H, m, cyclohexyl H1), 1.75–1.50 (5H, m, cyclohexyl equatorial), 1.24–1.04 (5H, m, cyclohexyl axial) ppm. ^{13}C NMR (DMSO-d_6) δ: 158.91, 156.81, 153.82, 144.52, 135.57, 131.25, 129.67, 128.59, 123.66, 120.73, 111.94, 72.56, 55.71, 49.46, 32.47, 25.08, 24.48 ppm. Anal. calc. for $C_{19}H_{23}N_3O_4$: C, 63.85; H, 6.49; N, 11.76, found: C, 64.09; H, 6.672; N, 11.68%; HRMS calc. for $C_{19}H_{24}N_3O_4$ [M + H]: 358.1767, found: 358.1768.

4.1.5.50. [3-(2-Methoxyphenyl)-6-oxopyridazin-1(6H)-yl]methyl heptylcarbamate, 16c. Crystallized from ethanol/water to yield 34.9%; m.p. 89 °C; ^{1}H NMR (DMSO-d_6) δ: 7.73 (1H, d, *J*: 10 Hz, pyridazine H5), 7.47–7.38 (3H, m, NH, phenyl H4,6), 7.15 (1H, d, *J*: 8 Hz, phenyl H3), 7.04 (1H, td, J_1: 7.6 Hz, J_2: 0.8 Hz, phenyl H5), 6.98 (1H, d, *J*: 9.6 Hz, pyridazine H4), 5.90 (2H, s, CH_2), 3.81 (3H, s, OCH_3), 2.94 (2H, q, CH_2), 1.37–1.34 (2H, m, CH_2), 1.23–1.20 (8H, m, CH_2), 0.82 (3H, t, CH_3) ppm; ^{13}C NMR (DMSO-d_6) δ: 158.89, 156.80, 154.65, 144.50, 135.56, 131.24, 129.65, 128.59, 123.66, 120.71, 111.94, 72.56, 55.70, 40.20, 31.16, 29.18, 28.32, 26.10, 21.98, 13.88 ppm; Anal. calc. for $C_{20}H_{27}N_3O_4$: C, 64.32; H, 7.29; N, 11.25, found: C, 64.55; H, 7.352; N, 11.27%; HRMS calc. for $C_{20}H_{28}N_3O_4$ [M + H]: 374.2080, found: 374.2066.

4.1.5.51. [3-(2-Methoxyphenyl)-6-oxopyridazin-1(6H)-yl]methyl dimethylcarbamate, 17c. The crude product was purified by preparative TLC using dichloromethane-methanol (100:3) solvent system. Yield 33.9%; m.p. 100 °C; ^{1}H NMR (DMSO-d_6) δ: 7.75 (1H, d, *J*: 9.6 Hz, pyridazine H5), 7.44 (2H, d, *J*: 7.6 Hz, phenyl H4,6), 7.15 (1H, d, *J*: 8 Hz, phenyl H3), 7.05 (1H, td, J_1: 7.6 Hz, J_2: 0.8 Hz, phenyl H5), 6.98 (1H, d, *J*: 10 Hz, pyridazine H4), 5.93 (2H, s, CH_2), 3.82 (3H, s, OCH_3), 2.81 (3H, s, CH_3), 2.79 (3H, s, CH_3) ppm; ^{13}C NMR (DMSO-d_6) δ: 158.84, 156.79, 154.20, 144.50, 135.59, 131.26, 129.74, 128.65, 123.62, 120.77, 111.94, 73.70, 55.70, 36.01, 35.53 ppm; Anal. calc. for $C_{15}H_{17}N_3O_4{\cdot}H_2O$: C, 56.07; H, 5.96; N, 13.08, found: C, 56.13; H, 5.525; N, 12.80%; HRMS calc. for $C_{15}H_{18}N_3O_4$ [M + H]: 304.1297, found: 304.1293.

4.2. Cholinesterase inhibition assay

AChE and BuChE (inhibitory%) activities of the synthesized compounds were determined by the modified Ellman's method [21–23]. Electric eel AChE (type-VI-S, EC 3.1.1.7), equine BuChE (EC 3.1.1.8), acetylthiocholine iodide, butyrylthiocholine chloride, 5,5′-dithio-bis-(2-nitrobenzoic acid) (DTNB), donepezil hydrochloride, and galantamine hydrobromide were purchased from Sigma-Aldrich. The assay was carried out by VersaMax Molecular Devices microplate reader.

For AChE inhibitory assay; 140 µL of 0.1 mM sodium phosphate buffer (pH = 8), 20 µL of test solution and 20 µL of AChE (0.2 unit/mL) solution were added in a 96-well microplate. After 10 min preincubation at room temperature, 10 µL of DTNB (10 mM) was added into each well followed by 10 µL of acetylthiocholine iodide (0.4 mM). Absorbance of the yellow end product was measured at 412 nm utilizing a 96-well microplate reader. Percentage of inhibition of AChE was determined by comparison of rates of reaction of samples relative to blank sample (ethanol in phosphate buffer pH = 8) using the formula $(E\text{-}S)/E \times 100$, where *E* is the activity of enzyme without test sample and *S* is the activity of enzyme with test sample. The experiments were done in quadruplicate and the results were expressed as average values with SD (Standard Deviation). For BuChE inhibitory assay, the same procedure as described above was followed except for the use of enzyme and substrate, which were BuChE (0.4 unit/mL) and butyrylthiocholine chloride (0.2 mM), respectively. Compounds displayed more than 50% inhibition were tested for IC_{50} determination. Each IC_{50} value was calculated by non-linear regression analysis using the GraphPad Prism program and determined from at least two independent experiments.

4.3. Time-dependent inhibition assay

Time-dependent inhibition of eqBuChE was studied using IC_{50} shift approach [32–34]. In this assay, the IC_{50} values of the selected compounds (**7c**, **14c**, and **16c**) and reference (rivastigmine, pseudo-irreversible inhibitor) were determined by three different pre-incubation times (10, 20, 40 min). Briefly; test compounds (20 µL) were allowed to pre-incubate with eqBuChE (20 µL, 0.4 unit/mL) for various periods of time in 140 µL of 0.1 mM sodium phosphate buffer (pH = 8) at room temperature. Following the pre-incubation step, the substrate butyrylthiocholine chloride (10 µL, 0.2 mM) and DTNB (10 µL, 10 mM) were added to the incubation mixture and the change in the absorbance was recorded. All measurements were carried out in triplicate and were expressed as mean ± SD. The IC_{50} values were calculated using GraphPad Prism software.

4.4. Kinetic studies of cholinesterase inhibition

To investigate the mechanism of action of the selected compounds (**7c**, **14c**, **16c**) on BuChE, a kinetic analysis was performed by using Ellman's method [35–37]. The experiments were carried out by varying the concentration of the substrate (butyrylthiocholine chloride, from 0.013 mM to 0.054 mM) in the presence of different concentration of

the inhibitors (**7c** and **14c**: 100 μM, 50 μM, 10 μM, 5 μM; **16c**: 50 μM, 10 μM, 5 μM, 1 μM). Mode of inhibition of the enzyme was assayed by Lineweaver-Burk plot of the inverse of the velocities (1/V) versus the inverse of the substrate concentration 1/[S] (mM^{-1}). Slopes of the reciprocal plots were then plotted against the concentration of inhibitor, for estimation of K_i. All processes were assayed in triplicate.

4.5. Molecular docking

The molecular docking studies were carried out using Glide and Induced fit docking protocols implemented in the Schrödinger Small-Molecule Drug Discovery Suite (Small-Molecule Drug Discovery Suite 2018-1, Schrödinger, LLC, New York, NY, 2018) with an iMac 3.2 GHz quad-core Intel Core i5 processor with 8 GB of memory on one CPU. The compounds which were built *via* builder panel in Maestro were subjected to ligand preparation by LigPrep (Schrödinger Release 2018-1: LigPrep, Schrödinger, LLC, New York, NY, 2018) using default conditions. The crystal structures of the *Ee*AChE (PDB:1C2O) [38], hAChE (PDB: 4EY7) [39] and the hBuChE (PDB: 4TPK) [40] were retrieved from the Protein Data Bank. The proteins were prepared using the Protein Preparation Wizard tool. Hydrogen atoms were added followed by assignment of all atom charges and atom types. Finally, energy minimization and refinement of the structures were done up to 0.3 Å RMSD by applying OPLS-2005 force field. Centroid of the active site residues was defined as the grid box. Van der Waals (vdW) radius scaling factor 1.00, partial charge cutoff 0.25, and OPLS-2005 force filed were used for receptor grid generation. The compounds prepared by LigPrep were docked into hBuChE using the extra-precision (XP) docking mode of the Glide without using any constraints and a 0.80 vdW radius scaling factor and 0.15 partial charge cutoff [41]. The protocol facilitates docking by ligand flexibility and generation of multiple conformers within the rigid receptor. The compounds prepared by LigPrep were docked into AChE using the IFD protocol [27] which considers flexibility to both compounds and receptor. The following residues ASP74, TRP86, TYR124, TYR133, SER203, TRP286, PHE295, PHE297, TRY337, PHE338 and HIS447 lining the binding site of AChE were kept as flexible. The initial docking protocol was set to employ a 0.50 vdW radius scaling factor and the resulting top 20 poses of each compound were taken. Extra-precision (XP) algorithm was employed in redocking of the compounds with the low energy refined structures generated by Prime MM-GBSA method. Best conformation for each compound was chosen based on the lowest XP glide score.

Acknowledgments

This work was supported by The Scientific and Technological Research Council of Turkey (TUBITAK) (grant number 117S872).

Declaration of Competing Interest

The authors declare no conflict of interest.

References

[1] Towards a dementia plan: a WHO guide. Geneva: World Health Organization, 2018.
[2] World Alzheimer Report, 2018. The state of the art of dementia research: New frontiers. London: Alzheimer's Disease International (ADI), 2018.
[3] J.M. Garcia-Alberca, P. Lara Munoz, M. Berthier Torres, Neuropsychiatric and behavioral symptomatology in Alzheimer's disease, Actas. Esp. Psiquiatr. 38 (4) (2010) 212–222.
[4] C.G. Lyketsos, M.C. Carrillo, J.M. Ryan, A.S. Khachaturian, P. Trzepacz, J. Amatniek, J. Cedarbaum, R. Brashear, D.S. Miller, Neuropsychiatric symptoms in Alzheimer's disease, Alzheimers Dement. 7 (2011) 532–539.
[5] Alzheimer's Association. 2019 Alzheimer's Disase Facts and Figures. Alzheimers Dement., 15(3) (2019) 321–387.
[6] X. Du, X. Wang, M. Geng, Alzheimer's disease hypothesis and related therapies, Transl. Neurodeg. 7 (2) (2018), https://doi.org/10.1186/s40035-018-0107-y.
[7] C.A. Lane, J. Hardy, J.M. Schott, Alzheimer's disease, Eur. J. Neurol. 25 (2018) 59–70.
[8] A. Kumar, A.E. Singh, A review on Alzheimer's disease pathophysiology and its management: an update, Pharmacol. Rep. 67 (2015) 195–203.
[9] Q. Li, S. He, Y. Chen, F. Feng, W. Qu, H. Sun, Donepezil-based multi-functional cholinesterase inhibitors for treatment of Alzheimer's disease, Eur. J. Med. Chem. 158 (2018) 463–477.
[10] Q. Li, H. Yang, Y. Chen, H. Sun, Recent progress in the identification of selective butyrylcholinesterase inhibitors for Alzheimer's disease, Eur. J. Med. Chem. 132 (2017) 294–309.
[11] U. Kosak, B. Brus, D. Knez, S. Zakelj, J. Trontelj, A. Pislar, R. Sink, M. Jukic, M. Zivin, A. Podkowa, F. Nachon, X. Brazzolotto, J. Stojan, J. Kos, N. Coquelle, K. Salat, J.P. Colletier, S. Gobec, The magic of crystal structure-based inhibitor optimization: development of a butyrylcholinesterase inhibitor with picomolar affinity and *in vivo* activity, J. Med. Chem. 61 (2018) 119–139.
[12] I.R. Macdonald, S.P. Maxwell, G.A. Reid, M.K. Cash, D.R. DeBay, S. Darvesh, Quantification of butyrylcholinesterase activity as a sensitive and specific biomarker of Alzheimer's disease, J. Alzheimers Dis. 58 (2017) 491–505.
[13] S. Darvesh, M.K. Cash, A. Reid, E. Martin, A. Mitnitski, C. Geula, Butyrylcholinesterase is associated with beta-amyloid plaques in the transgenic APPswe/PSEN1dE9 mouse model of Alzheimer disease, J. Neuropathol. Exp. Neurol. 71 (1) (2012) 2–14.
[14] A. Kumar, F. Pintus, A. Di Petrillo, R. Medda, P. Caria, M.J. Matos, D. Vina, E. Pieroni, F. Delogu, B. Era, G.L. Delogu, A. Fais, Novel 2-phenylbenzofuran derivatives as selective butyrylcholinesterase inhibitors for Alzheimer's disease, Sci. Rep. 8 (2018) 4424.
[15] M. Bajda, K. Latka, M. Hebda, J. Jonczyk, B. Malawska, Novel carbamate derivatives as selective butyrylcholinesterase inhibitors, Bioorg. Chem. 78 (2018) 29–38.
[16] Ş. Urlu-Çiçekli, Design and activity evaluation of compounds with acetylcholinesterase inhibitory activity against Alzheimer's disease, PhD Thesis, Gazi University, Institute of Health Sciences, 2017.
[17] J. Takahashi, I. Hijikuro, T. Kihara, M.G. Murugesh, S. Fuse, Y. Tsumura, A. Akaike, T. Niidome, T. Takahashi, H. Sugimoto, Design, synthesis and evaluation of carbamate-modified (-)-N1-phenethylnorphysostigmine derivatives as selective butyrylcholinesterase inhibitors, Bioorg. Med. Chem. Lett. 20 (2010) 1721–1723.
[18] G. Huang, B. Kling, F.H. Darras, J. Heilmann, M. Decker, Identification of a neuroprotective and selective butyrylcholinesterase inhibitor derived from the natural alkaloid evodiamine, Eur. J. Med. Chem. 81 (2014) 15–21.
[19] L. Jing, G. Wu, D. Kang, Z. Zhou, Y. Song, X. Liu, P. Zhan, Contemporary medicinal-chemistry strategies for the discovery of selective butyrylcholinesterase inhibitors, Drug Discov. Today 24 (2) (2019) 629–635.
[20] F.H. Darras, B. Kling, J. Heilmann, M. Decker, Neuroprotective tri- and tetracyclic BChE inhibitors releasing reversible inhibitors upon carbamate transfer, ACS Med. Chem. Lett. 3 (2012) 914–919.
[21] M. Kovarova, K. Komersa, S. Stepankova, P. Parik, A. Cagan, New method for the determination of the half inhibition concentration (IC_{50}) of cholinesterase inhibitors, Z. Naturforsch. 68c (2013) 133–138.
[22] G.L. Ellman, K.D. Courtney, V. Andres Jr., R.M. Featherstone, A new and rapid colorimetric determination of acetylcholinesterase activity, Biochem. Pharmacol. 7 (1961) 88–95.
[23] P. Zdrazilova, S. Stepankova, K. Komers, K. Ventura, A. Cegan, Half inhibition concentration of new cholinesterase inhibitors, Z. Naturforsch C. 59 (3–4) (2004) 293–296.
[24] S. Darvesh, K.V. Darvesh, R.S. McDonald, D. Mataija, R. Walsh, S. Mothana, O. Lockridge, E. Martin, Carbamates with differential mechanism of inhibition toward acetylcholinesterase and butyrylcholinesterase, J. Med. Chem. 51 (2008) 4200–4214.
[25] U. Kosak, B. Brus, D. Knez, R. Sink, S. Zakelj, J. Trontelj, A. Pislar, J. Slenc, M. Gobec, M. Zivin, L. Tratnjek, M. Perse, K. Salat, A. Podkowa, B. Filipek, F. Nachon, X. Brazzolotto, A. Wieckowska, B. Malawska, J. Stojan, I.M. Rescan, J. Kos, N. Coquelle, J.-P. Colletier, S. Gobec, Development of an in-vivo active reversible butyrylcholinesterase inhibitor, Sci. Rep. 6 (2016) 39495.
[26] Y. Xu, J.-P. Colletier, M. Weik, H. Jiang, J. Moult, I. Silman, J.L. Sussman, Flexibility of aromatic residues in the active-site gorge of acetylcholinesterase: X-ray versus molecular dynamics, Biophys. J. 95 (5) (2008) 2500–2511.
[27] K. Zou, H. Luo, J. Wang, N. Huang, Induced-fit docking and virtual screening for 8-hydroxy- 3-methoxy5H-pyrido [2,1-c] pyrazin-5-one derivatives as inducible nitric oxide synthase inhibitors, J. Chem. Pharm. Res. 6 (2014) 1187–1194.
[28] A. Saxena, A.M. Redman, X. Jiang, O. Lockridge, B.P. Doctor, Differences in active site gorge dimensions of cholinesterases revealed by binding of inhibitors to human butyrylcholinesterase, Biochemistry 36 (48) (1997) 14642–14651.
[29] Y. Chen, H. Lin, H. Yang, R. Tan, Y. Bian, T. Fu, W. Li, L. Wu, Y. Pei, H. Sun, Discovery of new acetylcholinesterase and butyrylcholinesterase inhibitors through structure- based virtual screening, RSC Adv. 7 (2017) 3429–3438.
[30] W.J. Coates, A. McKillop, One-pot preparation of 6-substituted 3(2H)-pyridazinones from ketones, Synthesis (1993) 334–342.
[31] Anon, Production of 6-arylpyridazin-3-ones, Research Disclosure, 1990. RD 311123 19900310.
[32] H.J. Burt, A. Galetin, J.B. Houston, IC50-based approaches as an alternative method for assessment of time-dependent inhibition of CYP3A4, Xenobiotica 40 (5) (2010) 331–343.
[33] I. Tcholakov, C.E. Grimshaw, L. Shi, A. Kiryanov, S.T. Murphy, C.J. Larson, A. Plonowski, J. Ermolieff, Time-dependent inhibition of PHD2, Bioscience Rep. 37 (2017) 1–8.
[34] S. Vazquez-Rodriguez, M. Wright, C.M. Rogers, A.P. Cribbs, S. Velupillai, M. Philpott, H. Lee, J.E. Dunford, K.V.M. Huber, M.B. Robers, J.D. Vasta, M.L. Thezenas, S. Bonham, B. Kessler, J. Bennett, O. Federov, F. Raynaud, A. Donovan, J. Blagg, V. Bavetsias, U. Oppermann, C. Bountra, A. Kawamura,

P.E. Brennan, Design, synthesis and characterization of covalent KDM5 inhibitors, Angew. Chem. Int. Ed. 58 (2019) 515–519.
[35] B. Kilic, H.O. Gulcan, F. Aksakal, T. Ercetin, N. Oruklu, E.U. Bagriacik, D.S. Dogruer, Design and synthesis of some new carboxamide and propanamide derivatives bearing phenylpyridazine as a core ring and the investigation of their inhibitory potential on *in-vitro* acetylcholinesterase and butyrylcholinesterase, Bioorg. Chem. 79 (2018) 235–249.
[36] Y. Li, X. Qiang, L. Luo, X. Yang, G. Xiao, Q. Liu, J. Ai, Z. Tan, Y. Deng, Aurone Mannich base derivatives as promising multifunctional agents with acetylcholinesterase inhibition, anti-beta-amyloid aggregation and neuroprotective properties for the treatment of Alzheimer's disease, Eur. J. Med. Chem. 126 (2017) 762–775.
[37] S.Y. Li, N. Jiang, S.S. Xie, K.D.G. Wang, X.B. Wang, L.Y. Kong, Design, synthesis and evaluation of novel tacrine-rhein hybrids as multifunctional agents for the treatment of Alzheimer's disease, Org. Biomol. Chem. 12 (2014) 801–814.
[38] Y. Bourne, J. Grassi, P.E. Bougis, P. Marchot, Conformational flexibility of the acetylcholinesterase tetramer suggested by x-ray crystallography, J. Biol. Chem. 274 (1999) 30370–30376.
[39] J. Cheung, M.J. Rudolph, F. Burshteyn, M.S. Cassidy, E.N. Gary, J. Love, M.C. Franklin, J.J. Height, Structures of human acetylcholinesterase in complex with pharmacologically important ligands, J. Med. Chem. 55 (2012) 10282–10286.
[40] B. Brus, U. Kosak, S. Turk, A. Pislar, N. Coquelle, J. Kos, J. Stojan, J.P. Colletier, S. Gobec, Discovery, biological evaluation, and crystal structure of a novel nanomolar selective butyrylcholinesterase inhibitor, J. Med. Chem. 57 (2014) 8167–8179.
[41] R.A. Friesner, R.B. Murphy, M.P. Repasky, L.L. Frye, J.R. Greenwood, T.A. Halgren, P.C. Sanschagrin, D.T. Mainz, Extra precision glide: docking and scoring incorporating a model of hydrophobic enclosure for protein-ligand complexes, J. Med. Chem. 49 (2006) 6177–6196.